[redacted] Copy 93
RM L57J28a

NACA

RESEARCH MEMORANDUM

INVESTIGATION OF THE STATIC LATERAL STABILITY AND AILERON CHARACTERISTICS OF A 0.067-SCALE MODEL OF THE BELL X-2 AIRPLANE AT MACH NUMBERS OF 2.29, 2.78, 3.22, AND 3.71

By Roger H. Fournier and H. Norman Silvers

Langley Aeronautical Laboratory
Langley Field, Va.

[redacted]

NATIONAL ADVISORY COMMITTEE
FOR AERONAUTICS

WASHINGTON

March 3, 1958

[redacted]

NATIONAL ADVISORY COMMITTEE FOR AERONAUTICS

RESEARCH MEMORANDUM

INVESTIGATION OF THE STATIC LATERAL STABILITY AND AILERON CHARACTERISTICS OF A 0.067-SCALE MODEL OF THE BELL X-2 AIRPLANE AT MACH NUMBERS OF 2.29, 2.78, 3.22, AND 3.71

By Roger H. Fournier and H. Norman Silvers

SUMMARY

Tests were performed in the high Mach number test section of the Langley Unitary Plan wind tunnel to determine the static lateral stability and aileron characteristics of a 0.067-scale model of the Bell X-2 airplane at Mach numbers of 2.29, 2.78, 3.22, and 3.71.

The results of this investigation indicated that the directional stability of the model was low with directional instability occurring at Mach numbers higher than 3.1 and angles of attack higher than about 5.0° (equivalent lift coefficient of about 0.18). The yaw due to aileron deflection was adverse and, with 10° of differential aileron deflection, large enough to overbalance the available directional restoring moment at all angles of attack higher than about 5.0° (equivalent lift coefficient of about 0.21) and Mach numbers higher than 2.5. The model also had positive effective dihedral for all test attitudes and Mach numbers. A combination of the lateral-stability parameters with the aileron characteristics to form a lateral-stability criterion for a maneuver using ailerons alone indicated that the model has characteristics which would give unstable aperiodic behavior (divergence) over a large part of the test Mach number and angle-of-attack range.

INTRODUCTION

In order to obtain information of use in the design of airplanes at moderate supersonic speeds, an investigation of static lateral stability and aileron characteristics of a 0.067-scale model of the Bell X-2 airplane at Mach numbers of 2.29, 2.78, 3.22, and 3.71 has been made in the

Langley Unitary Plan wind tunnel. A brief evaluation of the lateral stability and aileron characteristics of the model is presented. The present investigation extends the results obtained at lower supersonic speeds. (See refs. 1 to 3.)

COEFFICIENTS AND SYMBOLS

Data are presented about the stability system of axes. The lateral-stability data are also presented about the body system of axes. The system of axes and a diagram of the aileron deflection are shown in figure 1. Moment coefficients are referred to the quarter-chord of the mean aerodynamic chord.

C_L	lift coefficient, L/qS
C_D	drag coefficient, D/qS
C_{D_b}	base drag coefficient, $\frac{D_{base}}{qS}$
C_m	pitching-moment coefficient, $\frac{M_Y}{qSb}$
C_l	rolling-moment coefficient, $\frac{M_X}{qSb}$
C_n	yawing-moment coefficient, $\frac{M_Z}{qSb}$
C_Y	side-force coefficient, $\frac{F_Y}{qS}$
L	force along Z-axis
D	force along X-axis
M_Y	moment about Y-axis
M_X	moment about X-axis
M_Z	moment about Z-axis
F_Y	force along Y-axis
q	free-stream dynamic pressure, $0.7pM^2$, lb/sq ft
p	free-stream static pressure, lb/sq ft

M	free-stream Mach number
S	wing area including body intercept, sq ft
$\bar{c}$	wing mean aerodynamic chord, in.
$\bar{c}_t$	horizontal-tail mean aerodynamic chord, in.
b	wing span, in.
S_a	aileron area (one), sq ft
$\bar{c}_a$	aileron mean geometric chord, in.
α	angle of attack referred to X-axis (body reference line), deg
β	angle of sideslip referred to fuselage center line, deg
δ_a	aileron angle referred to chord perpendicular to the hinge line, positive when negative rolling moment is produced, deg
φ	roll angle of model, 0° with wing vertical
L/D	lift-drag ratio, C_L/C_D
$C_{D_{min}}$	minimum drag coefficient
C_{L_α}	lift-curve slope ($\beta = 0^\circ$), $\frac{\partial C_L}{\partial \alpha}$
$C_{m_{C_L}}$	pitching-moment-curve slope ($C_L = 0$), $\frac{\partial C_m}{\partial C_L}$
C_{n_β}	directional-stability parameter ($\beta = 0^\circ$), $\frac{\partial C_n}{\partial \beta}$
C_{l_β}	effective-dihedral parameter ($\beta = 0^\circ$), $\frac{\partial C_l}{\partial \beta}$
C_{Y_β}	side-force parameter ($\beta = 0^\circ$), $\frac{\partial C_Y}{\partial \beta}$
$C_{n_{\delta_a}}$	aileron yawing-moment parameter ($\delta_a = 0^\circ$), $\frac{\partial C_n}{\partial \delta_a}$
$C_{l_{\delta_a}}$	aileron effectiveness ($\delta_a = 0^\circ$), $\frac{\partial C_l}{\partial \delta_a}$

T58-5872

Subscripts:

w refers to the stability axis when used with yawing-moment coefficient

s refers to the stability axis

0 denotes value of parameter at zero lift coefficient

MODEL AND APPARATUS

The tests were conducted in the high Mach number test section of the Langley Unitary Plan wind tunnel. This tunnel is a variable-pressure, continuous, return-flow type. The test section is 4 feet square and approximately 7 feet in length. The nozzle leading to the test section is of the asymmetric sliding-block type, and variable Mach numbers may be obtained continuously through a Mach number range from approximately 2.29 to 4.65 without tunnel shutdown.

A three-view drawing of the model is shown in figure 2, and the geometric characteristics of the model are given in table I. The model had a wing with 40° sweepback of the quarter-chord line, an aspect ratio of 4.0, a taper ratio of 0.5, and 10-percent-thick circular-arc airfoil sections normal to the quarter-chord line. The wing had a 3° incidence angle with respect to the fuselage center line. Twenty-percent-chord flatsided ailerons having a trailing-edge thickness equal to 0.5 of the hinge-line thickness were installed on the outboard halves of the wing semispans. (See fig. 3.) Measurements indicated the right wing tip to be twisted 0.2° with respect to the left wing tip.

Forces and moments for the model were measured by means of a six-component internal strain-gage balance. This balance was attached, by means of a sting, to the tunnel central support system. Included in the model support system was a remotely operated adjustable-angle coupling that permitted tests to be made at variable angles of attack concurrently with variations in the angle of sideslip.

TESTS

Tests were made through an angle-of-attack range from approximately -4° to 12° at angles of sideslip of 0° and -5° to obtain aerodynamic characteristics in pitch and to obtain incremental information from which

lateral-stability parameters could be computed over the angle-of-attack range. At angles of attack of about 0°, 5°, and 10°, tests were made at angles of sideslip from -10° to 10° to obtain the lateral characteristics outside the angle-of-sideslip range where the lateral results were linear. All basic-model tests were made with a stabilizer deflection of -5°. Tests were made to determine aileron effectiveness at differential aileron angles of 0° and -10°. For an aileron deflection of -10°, the left aileron was deflected down 5°, and the right aileron was deflected up 5°.

The test conditions are listed in the following table:

M	Stagnation pressure, lb/sq in. abs	Dynamic pressure, lb/sq ft	Reynolds number
2.29	23.2	996.18	2.54×10^6
2.78	29.6	876.01	2.57
3.22	37.8	775.90	2.58
3.71	44.6	604.37	2.38

The Reynolds number is based on the mean geometric chord of the wing. The stagnation temperature was maintained at 150° F for all Mach numbers.

CORRECTIONS AND ACCURACY

No corrections have been applied to the data for stream angularity or buoyancy, inasmuch as the calibration of the test section has not been completed. Preliminary indications are that some flow angularity exists but the exact amount is not known. In the test section the longitudinal pressure gradients are felt to be small and produce negligible effects on the model.

The maximum deviation of local Mach number in the portion of the tunnel occupied by the model was ±0.015 from the average values listed in the test conditions. The angles of attack and sideslip have been corrected for the deflection of the support system under load. The axial force, before resolution into drag coefficient, was adjusted to a base pressure equal to the free-stream static pressure. The increment in axial-force coefficient used to make the adjustment has been converted to a drag coefficient and is shown in figure 4 as a function of angle of attack for the four test Mach numbers.

The estimated accuracy of the individual measured quantities is as follows:

C_L	±0.004
C_D	±0.0010
C_m	±0.002
C_l	±0.0005
C_n	±0.0025
C_Y	±0.0025
α, deg	±0.1
β, deg	±0.1
δ_a, deg	±0.1

Based on the accuracy of the above coefficients and angles and the values of the parameters measured, the estimated accuracy of the lateral-stability parameters computed from increments in coefficients and angles is:

C_{Y_β}	±0.0014
C_{n_β}	±0.0004
C_{l_β}	±0.0004

PRESENTATION OF RESULTS

The results of this investigation are presented in the following figures:

The angles of attack given in the lateral-stability results (figs. 7 to 14) are the values at an angle of sideslip of 0° corrected for deflection of the support system under load.

DISCUSSION

The basic longitudinal aerodynamic characteristics are presented in figure 6 and are summarized in figure 15. No discussion of the characteristics shown by these data is included in this paper. The lateral-stability results are presented for two axes systems (body and stability) for the convenience of those wishing to compare dynamic-stability estimations utilizing different axes systems.

The lateral-stability results on the stability axes are summarized in figure 16. Comparison of the basic results in the two axes systems reveals the usual transfer effect of angle of attack on the yawing-moment coefficient, that is, the directional stability of the model on the stability axis is increased over that on the body axis as the angle of attack is increased. For discussion purposes, only the results in the stability system of axes will be used. These results (figs. 11 to 14) show that the lateral-stability coefficients vary linearly within the range of sideslip angles from 0° to at least -5°. The lateral parameters presented in the summary results (fig. 16) and computed from runs made at angles of sideslip of 0° and about -5° (represented by the faired curves) are therefore a good representation of the linearized characteristics of the model.

The directional-stability characteristics as well as other parameters presented herein compare well with the results obtained earlier at low supersonic Mach numbers (refs. 1, 2, and 3). The directional-stability results of the present test when compared with those of previous tests show the usual reduction with an increase in Mach number. This reduction is due to the effect of Mach number on the vertical-tail lift-curve slope and to dynamic pressure at the tail. Although the directional stability of the model in the present test is low, it is stable at an angle of attack of 0° at all Mach numbers. Directional instability occurs at an

angle of attack of approximately 5.0° ($C_L \approx 0.18$) at a Mach number of 3.1. At an angle of attack of 10° ($C_L \approx 0.34$) directional instability occurs at a Mach number of about 2.9. The model has positive effective dihedral $\left(-C_{l_\beta}\right)$ throughout the test Mach number and angle-of-attack range.

The summary of the lateral characteristics (fig. 16) also shows that the yawing-moment coefficient due to a 5° deflection of each aileron (differential deflection of 10°) is adverse and is large enough to overbalance the stabilizing moment of the model at all angles of attack greater than 5.0° and Mach numbers higher than approximately 2.5. (See figs. 11 to 14.) The combination of low directional stability, positive effective dihedral, and relatively high adverse yaw due to aileron deflection when coupled with the rolling moment due to aileron deflection that exists can result in an airplane with undesirable lateral dynamic characteristics in this Mach number range. An index to the lateral behavior of the airplane is presented in figure 17. The criterion presented combines the aileron characteristics with the lateral-stability parameters to indicate whether the combination of aerodynamic conditions will result in stable behavior or unstable aperiodic behavior of the configuration for a maneuver performed with the ailerons alone. For stability, the term $C_{l,s_\beta} C_{n,w_{\delta a}} - C_{n,w_\beta} C_{l,s_{\delta a}}$ must be positive. The results indicate that, at all angles of attack greater than 4° and Mach numbers greater than about 2.6, the existing lateral aerodynamic parameters in combination with the aileron characteristics will result in unstable aperiodic behavior of the configuration. This criterion does not consider the effect of corrective rudder deflection on the airplane behavior. Since rudder data are not available, it is not possible to present in this paper an evaluation of the effect of the rudder. It is possible to observe, however, that application of corrective rudder deflection could result in a controllable condition although unstable aperiodic lateral behavior exists. It is emphasized that the estimation of the expected degree of lateral maneuvering difficulty requires a complete dynamic analysis including the effect of rudder deflection (if rudder is used) and such other factors as aerodynamic damping and airplane inertia characteristics.

CONCLUSIONS

The results of an investigation of the lateral stability and aileron characteristics of a 0.067-scale model of the Bell X-2 airplane in the Langley Unitary Plan wind tunnel at Mach numbers of 2.29, 2.78, 3.22, and 3.71 indicate the following conclusions:

1. The directional stability of the model is low as was expected from earlier research on this configuration, instability occurring at Mach numbers higher than 3.1 and at angles of attack higher than about 5.0° (equivalent to a lift coefficient of about 0.18).

2. The adverse yawing moment due to aileron deflection is large enough with 10° of differential deflection to overbalance the available directional restoring moment with the rudder undeflected at Mach numbers higher than about 2.5 and angles of attack higher than about 5.0° (equivalent to a lift coefficient of about 0.21).

3. The model has positive effective dihedral at all test Mach numbers and angles of attack.

4. A combination of lateral-stability parameters with the aileron characteristics to form a lateral-stability criterion for a maneuver using ailerons alone indicated that the model has characteristics which would give unstable aperiodic behavior over most of the range of Mach number and angle of attack.

Langley Aeronautical Laboratory,
National Advisory Committee for Aeronautics,
Langley Field, Va., October 8, 1957.

REFERENCES

1. Spearman, M. Leroy: An Investigation of a Supersonic Aircraft Configuration Having a Tapered Wing With Circular-Arc Sections and 40° Sweepback - Static Lateral Stability Characteristics at Mach Numbers of 1.40 and 1.59. NACA RM L50C17, 1950.

2. Spearman, M. Leroy, and Robinson, Ross B.: The Aerodynamic Characteristics of a Supersonic Aircraft Configuration With a 40° Sweptback Wing Through a Mach Number Range From 0 to 2.4 As Obtained From Various Sources. NACA RM L52A21, 1952.

3. Spearman, M. Leroy, and Palazzo, Edward B.: An Investigation of a Supersonic Aircraft Configuration Having a Tapered Wing With Circular-Arc Sections and 40° Sweepback - Static Longitudinal and Lateral Stability and Control Characteristics at a Mach Number of 1.89. NACA RM L54G26a, 1954.

TABLE I.- GEOMETRIC CHARACTERISTICS OF MODEL

Wing:	
Area, sq ft	1.158
Span, ft	2.155
Aspect ratio	4
Sweepback of quarter-chord line, deg	40
Taper ratio	0.5
Mean aerodynamic chord, ft	0.557
Airfoil section normal to quarter-chord line	10-percent-thick, circular arc
Twist, deg	0
Dihedral, deg	3
Horizontal tail:	
Area, sq ft	0.196
Span, ft	0.855
Aspect ratio	3.72
Sweepback of quarter-chord line, deg	40
Taper ratio	0.5
Airfoil section	NACA 65-008
Vertical tail:	
Area (exposed), sq ft	0.172
Aspect ratio (based on exposed area and span)	1.17
Sweepback of leading edge, deg	40.6
Taper ratio	0.337
Airfoil section, root	NACA 27-010
Airfoil section, tip	NACA 27-008
Fuselage:	
Fineness ratio (canopies being neglected)	9.4
Miscellaneous:	
Tail length from $\bar{c}/4$ of wing to $\bar{c}_t/4$ of tail, ft	0.917
Tail height, wing semispans above fuselage center line	0.153

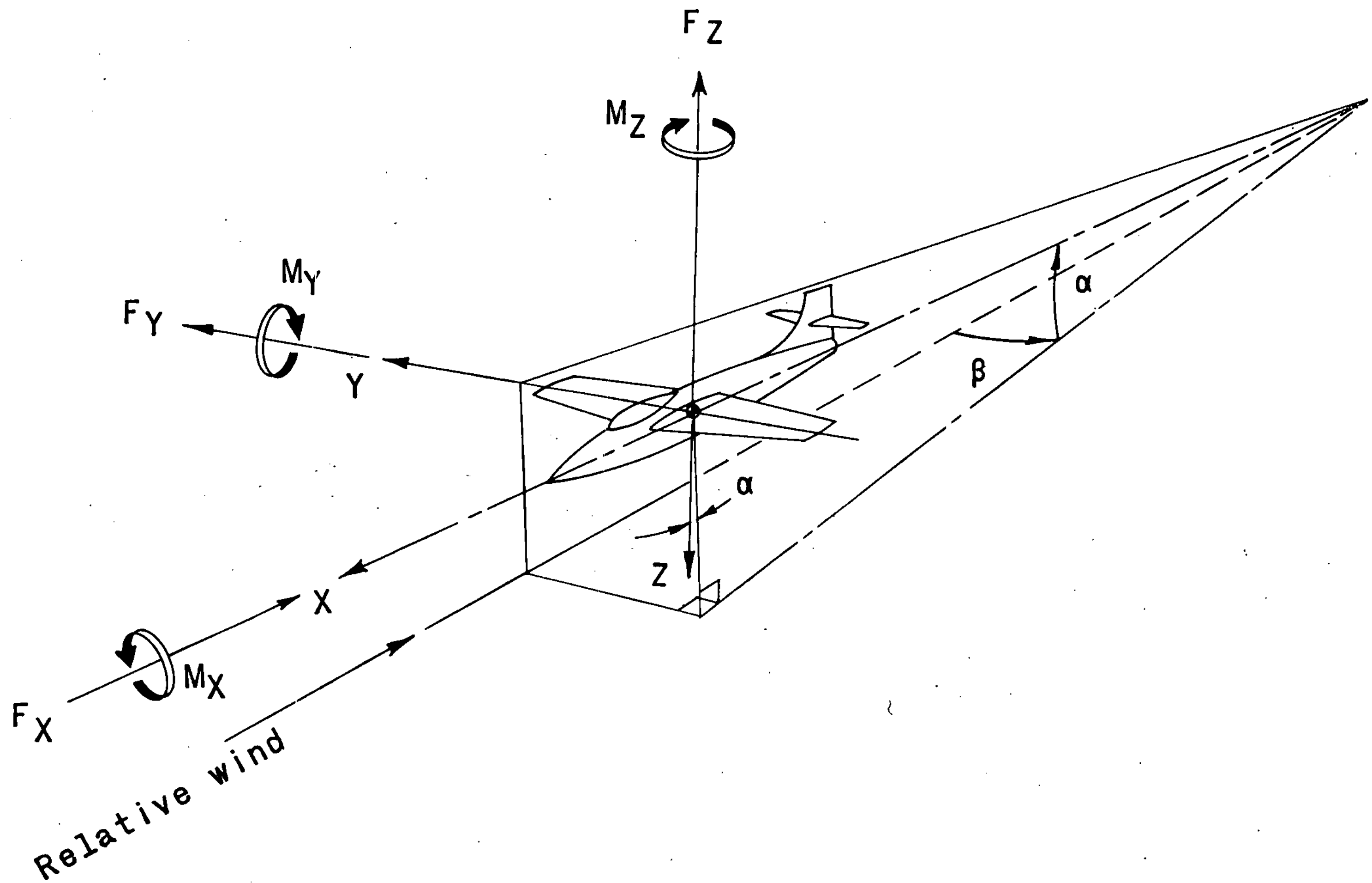

(a) Body axis.

Figure 1.- System of axes and diagram of control-surface deflections. Arrows indicate positive values.

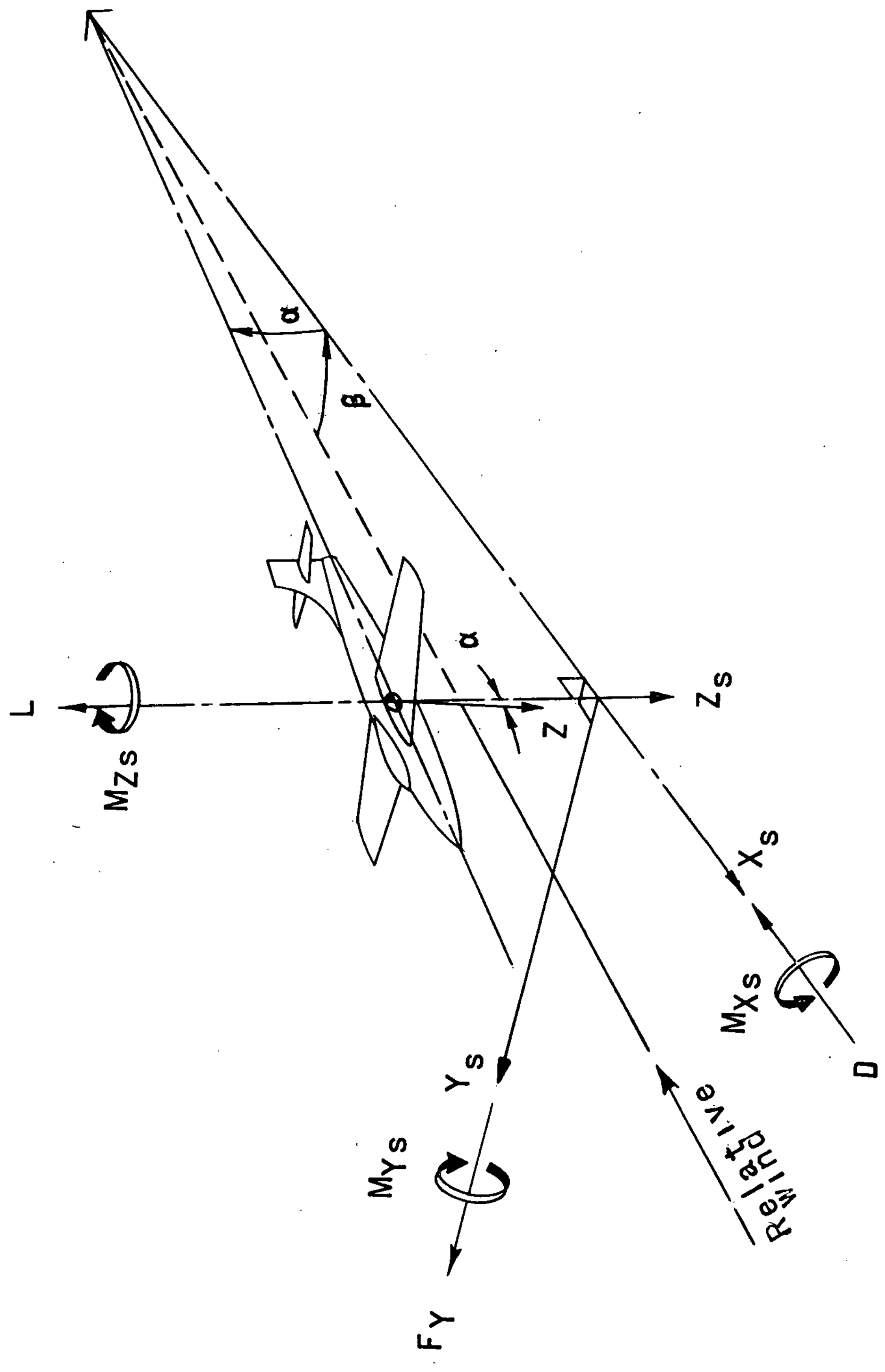

(b) Stability axis.

Figure 1.- Continued.

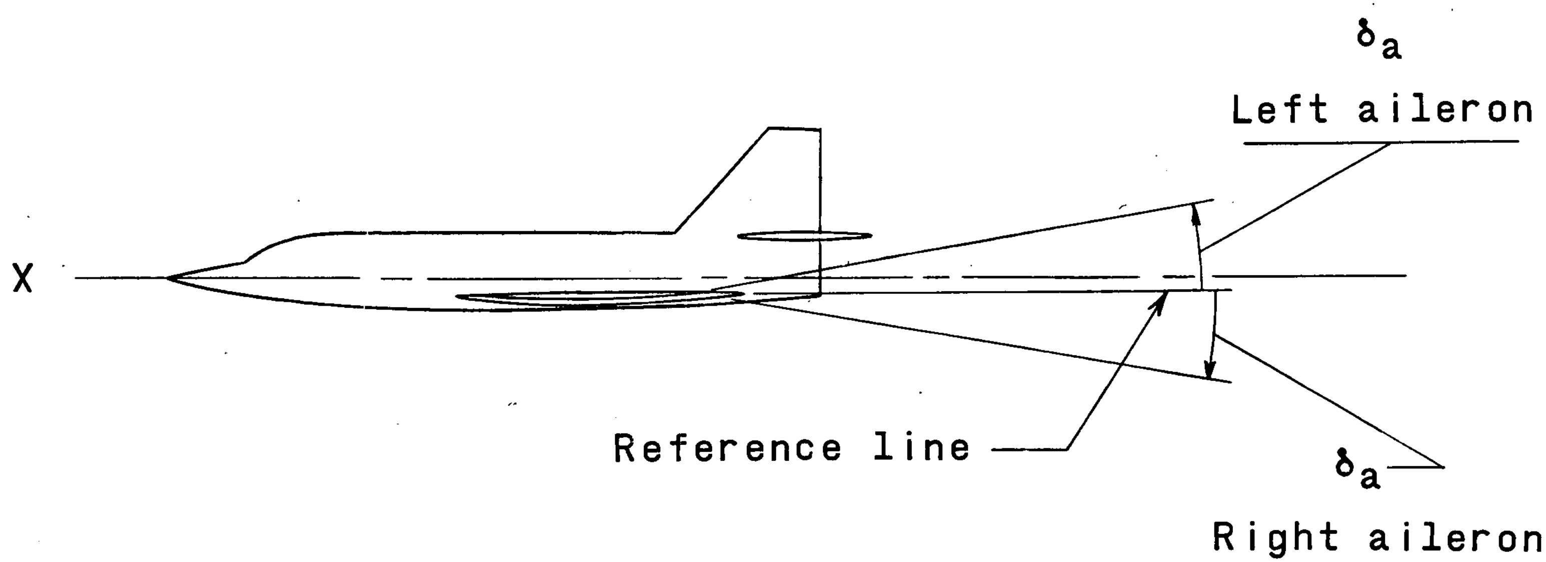

(c) Control-surface deflections. (Control-surface reference line is parallel to X-axis.)

Figure 1.- Concluded.

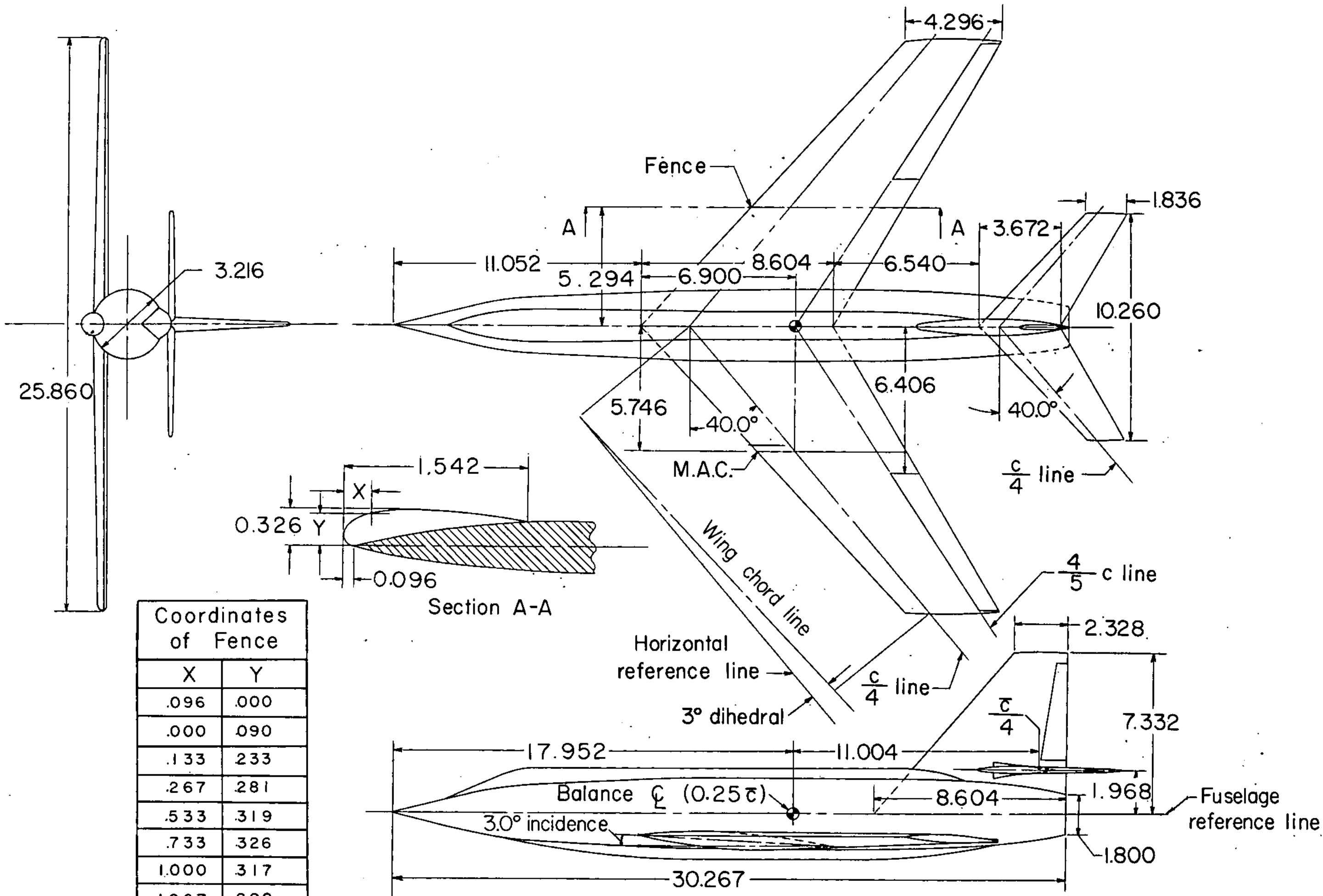

Coordinates of Fence	
X	Y
.096	.000
.000	.090
.133	.233
.267	.281
.533	.319
.733	.326
1.000	.317
1.267	.290
1.533	.183

Figure 2.- Details of the 0.067-scale model of the Bell X-2 airplane. Dimensions are in inches unless otherwise noted.

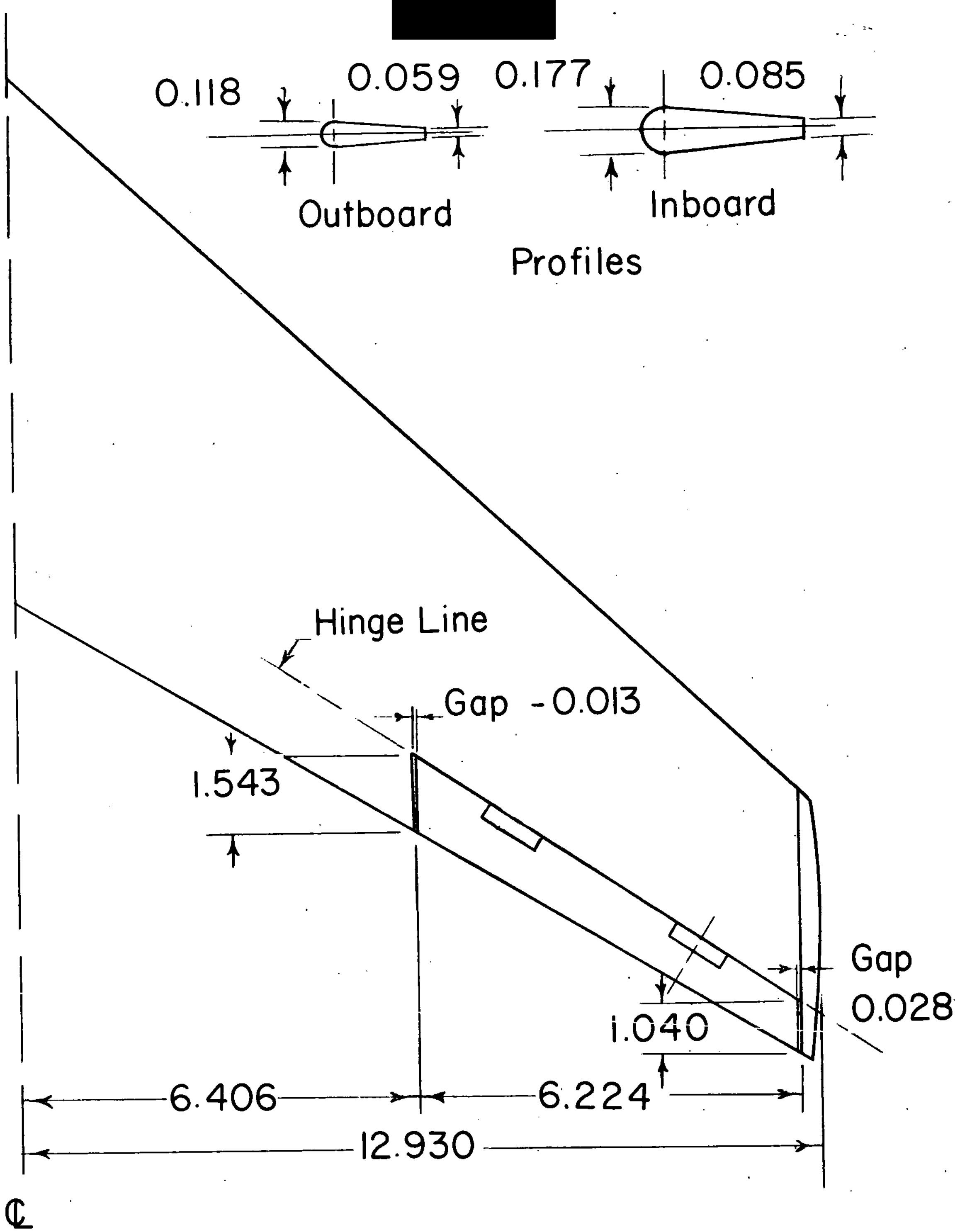

Figure 3.- Aileron details of the 0.067-scale model of the Bell X-2 airplane. All dimensions are in inches.

[redacted]

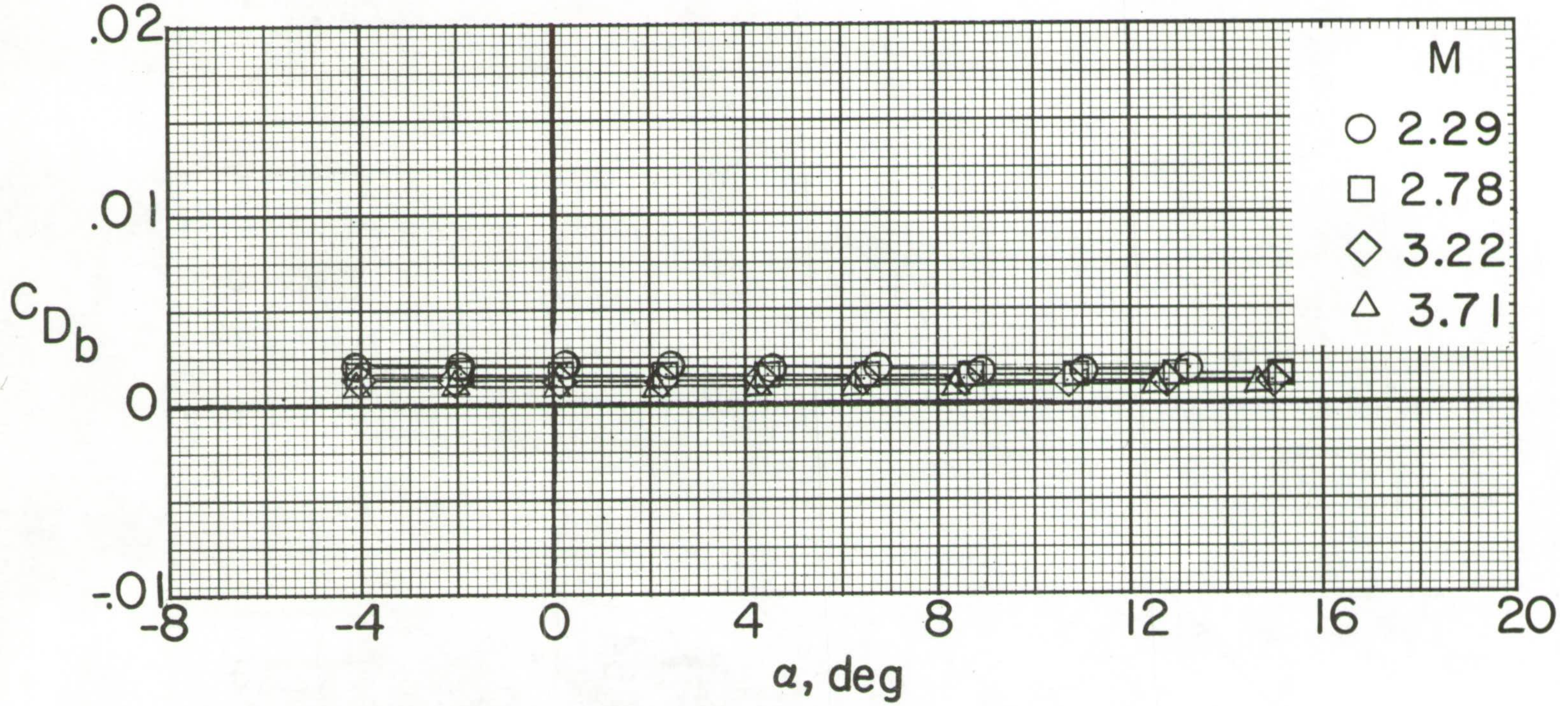

Figure 4.- Variation of the base drag coefficient with angle of attack for the 0.067-scale model of the Bell X-2 airplane.

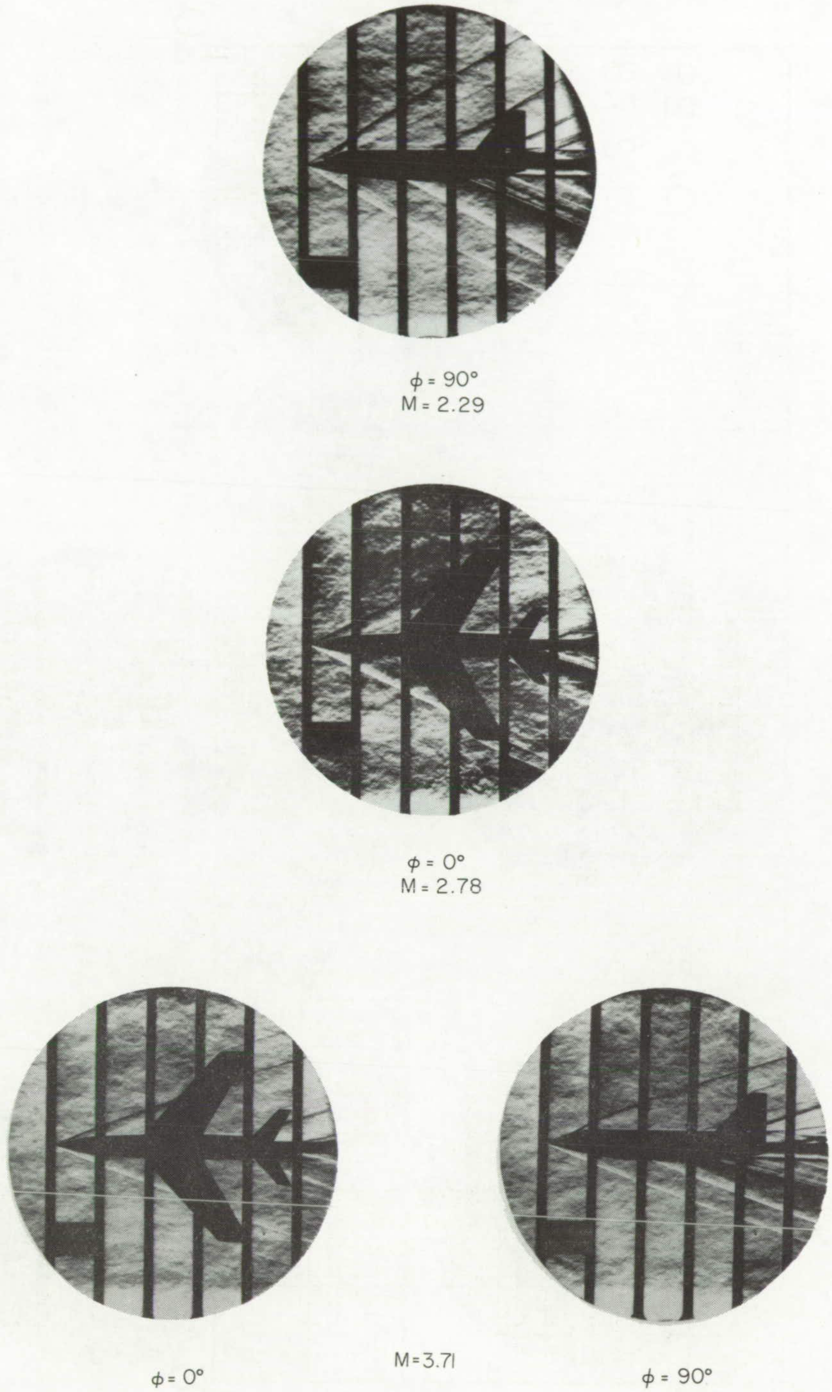

(a) $\delta_a = 0^\circ$. L-57-2794

Figure 5.- Schlieren photographs of the 0.067-scale model of the Bell X-2 airplane in the Langley Unitary Plan wind tunnel. $\alpha \approx 0^\circ$; $\beta \approx 0^\circ$.

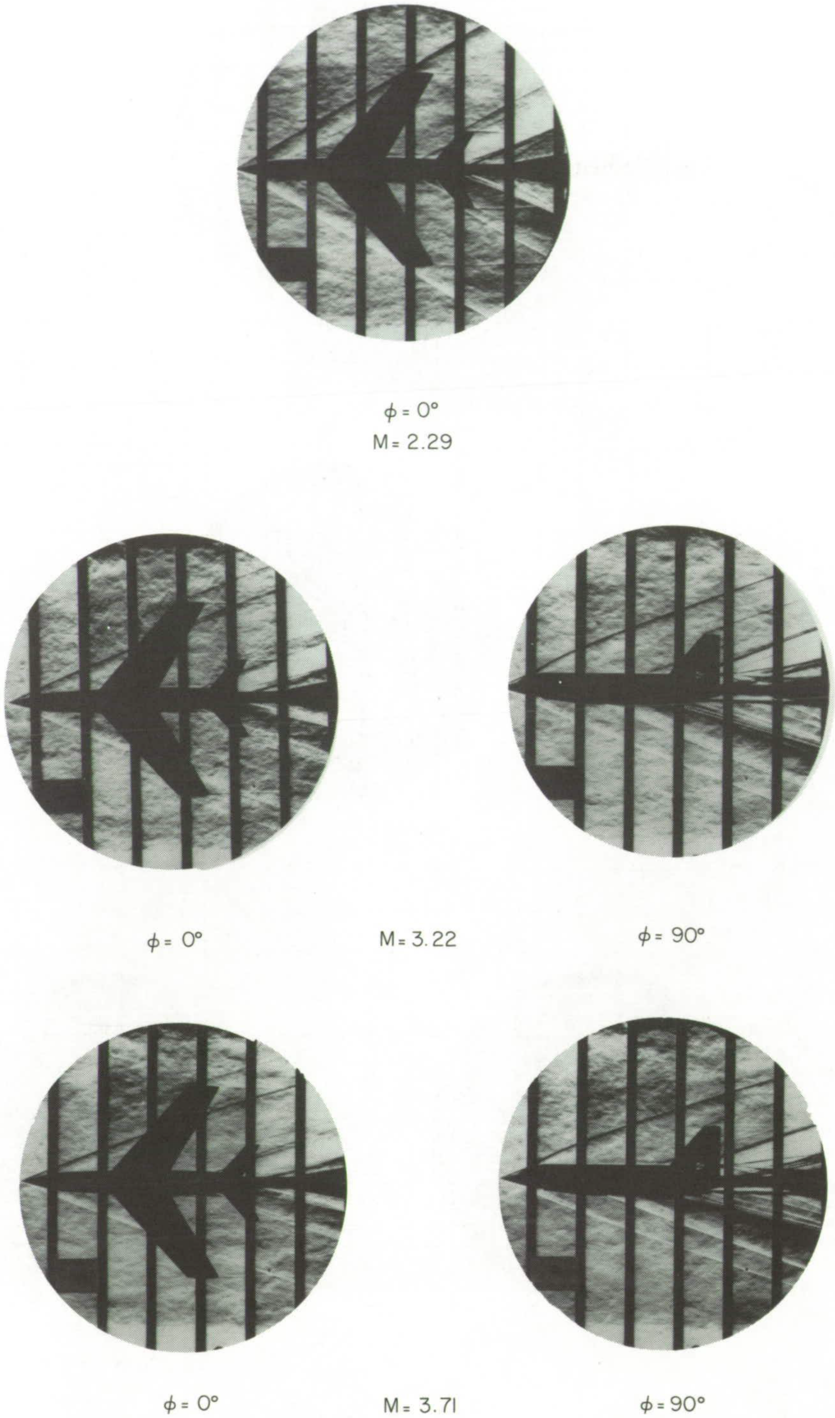

(b) $\delta_a = -10.0^{\circ}$. L-57-2795

Figure 5.- Concluded.

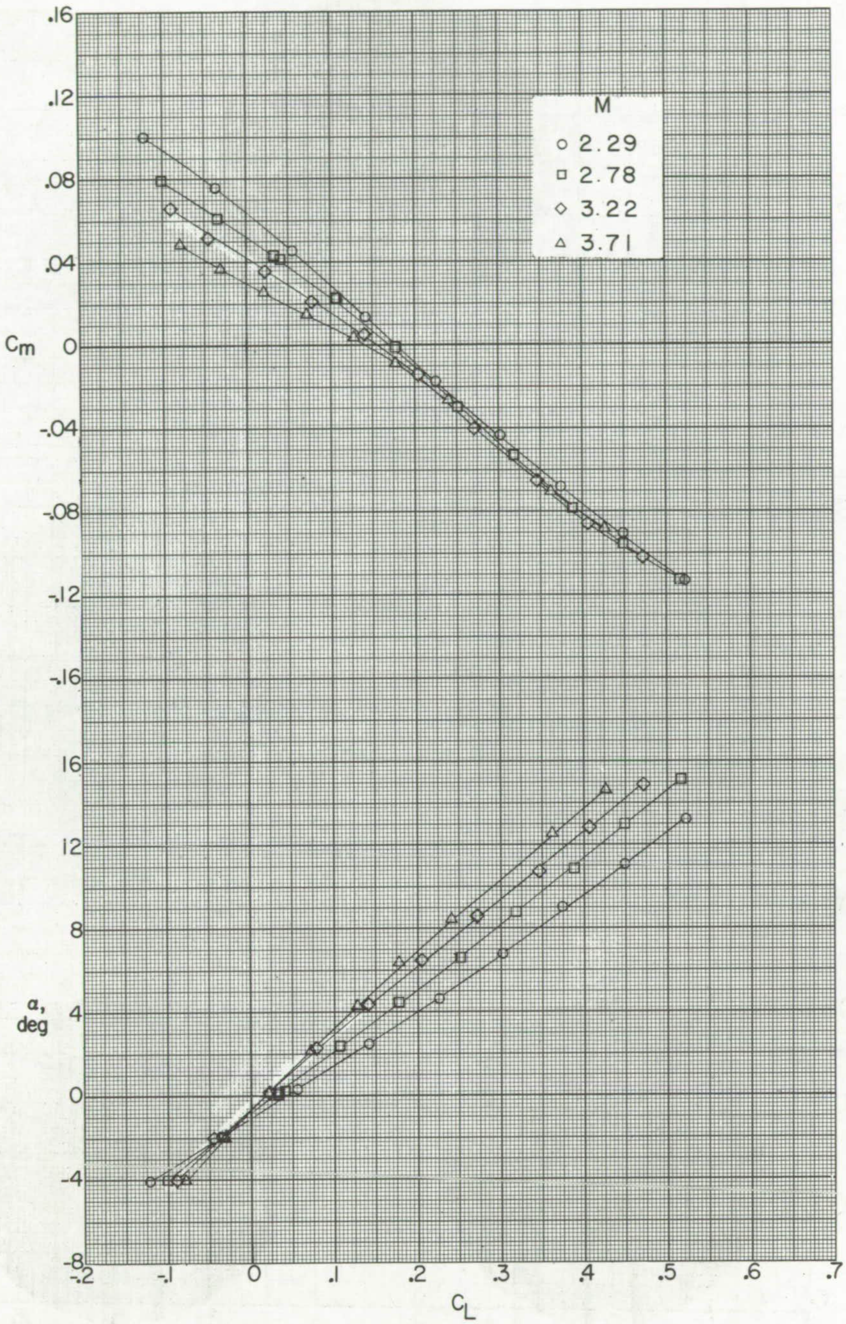

(a) $\delta_a = 0^{\circ}$.

Figure 6.- Aerodynamic characteristics in pitch of the 0.067-scale model of the Bell X-2 airplane.

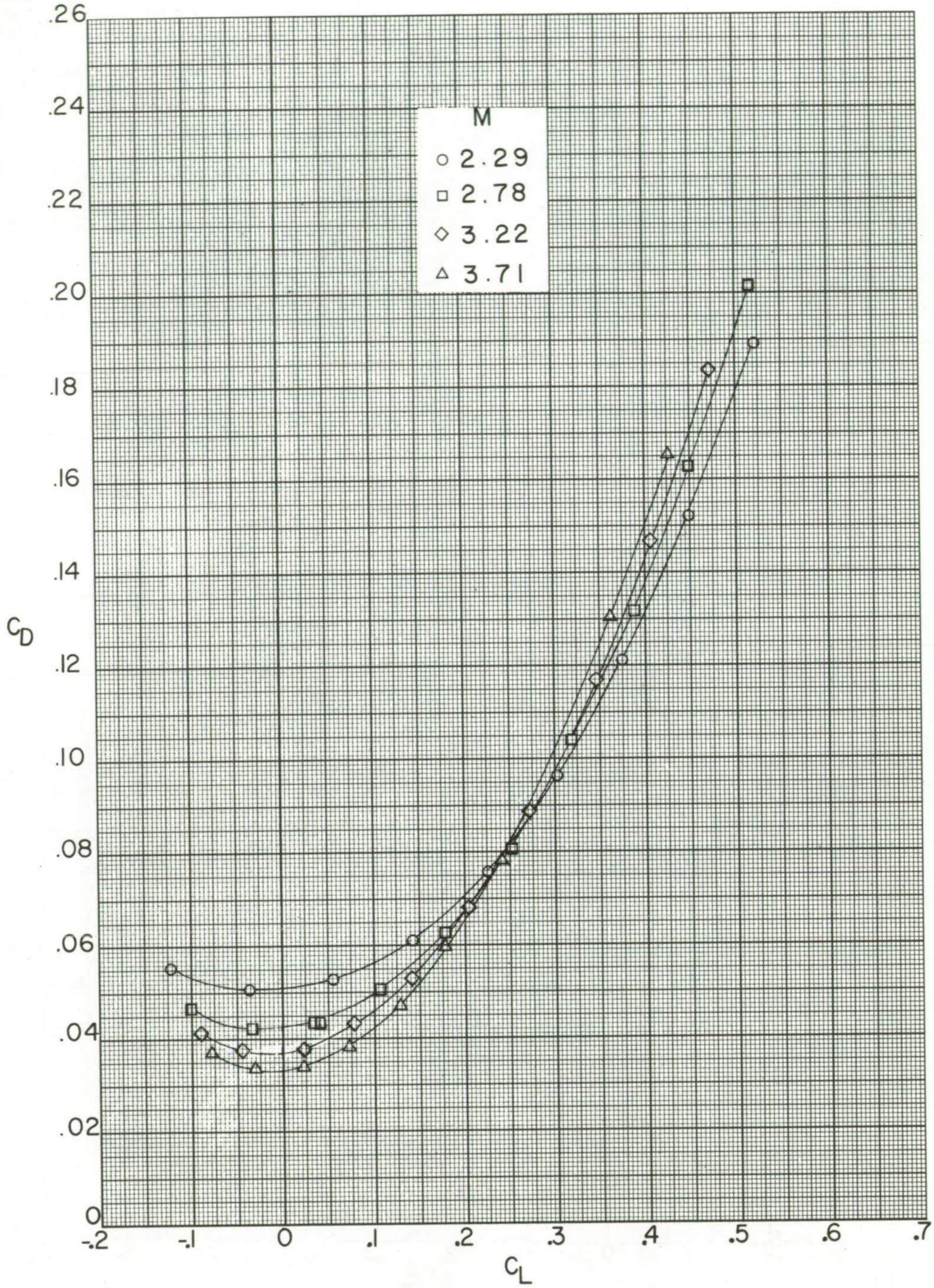

(a) Concluded.

Figure 6.- Continued.

[redacted]

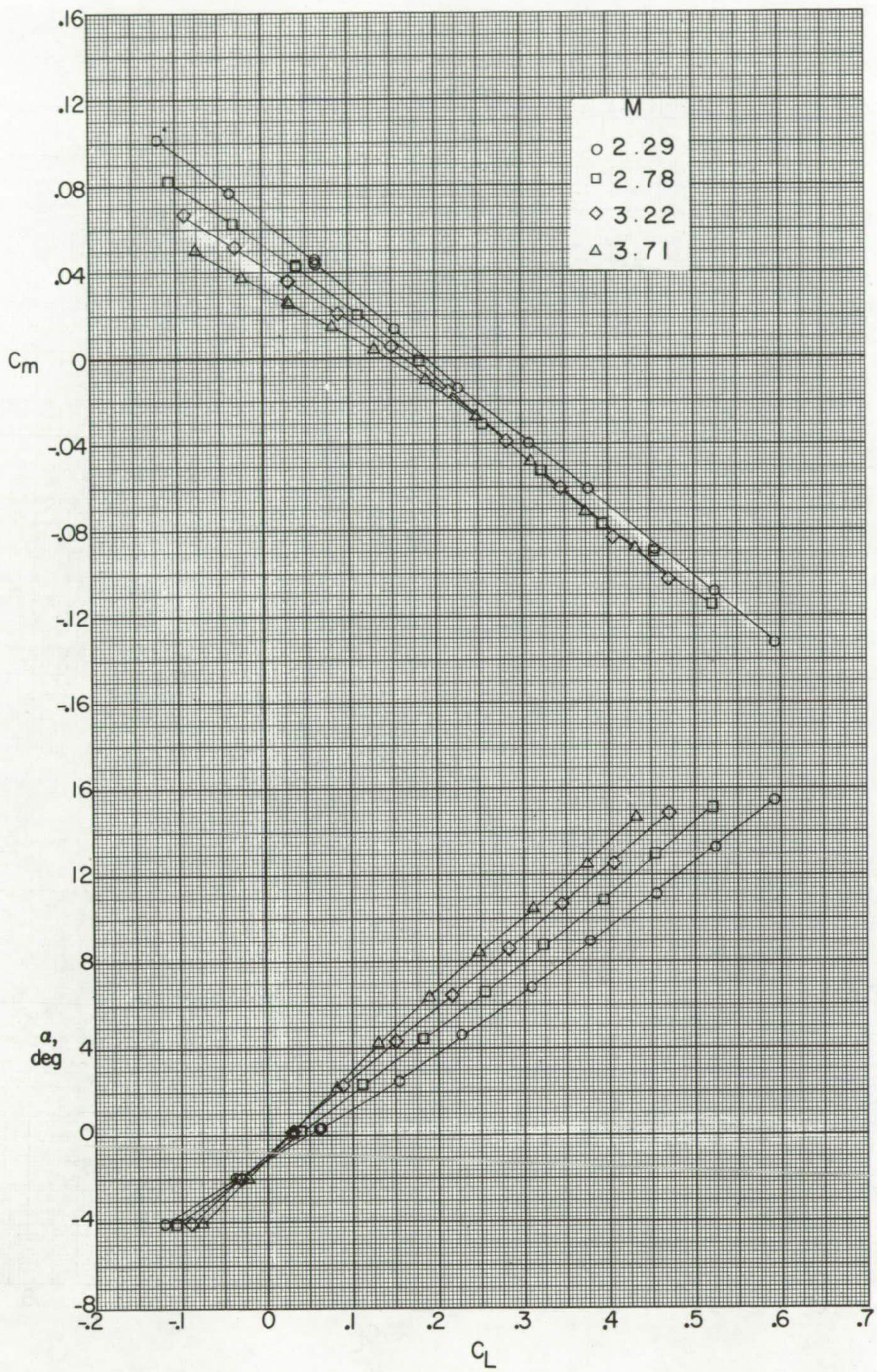

(b) $\delta_a = -10.0^{\circ}$.

Figure 6.- Continued.

[redacted]

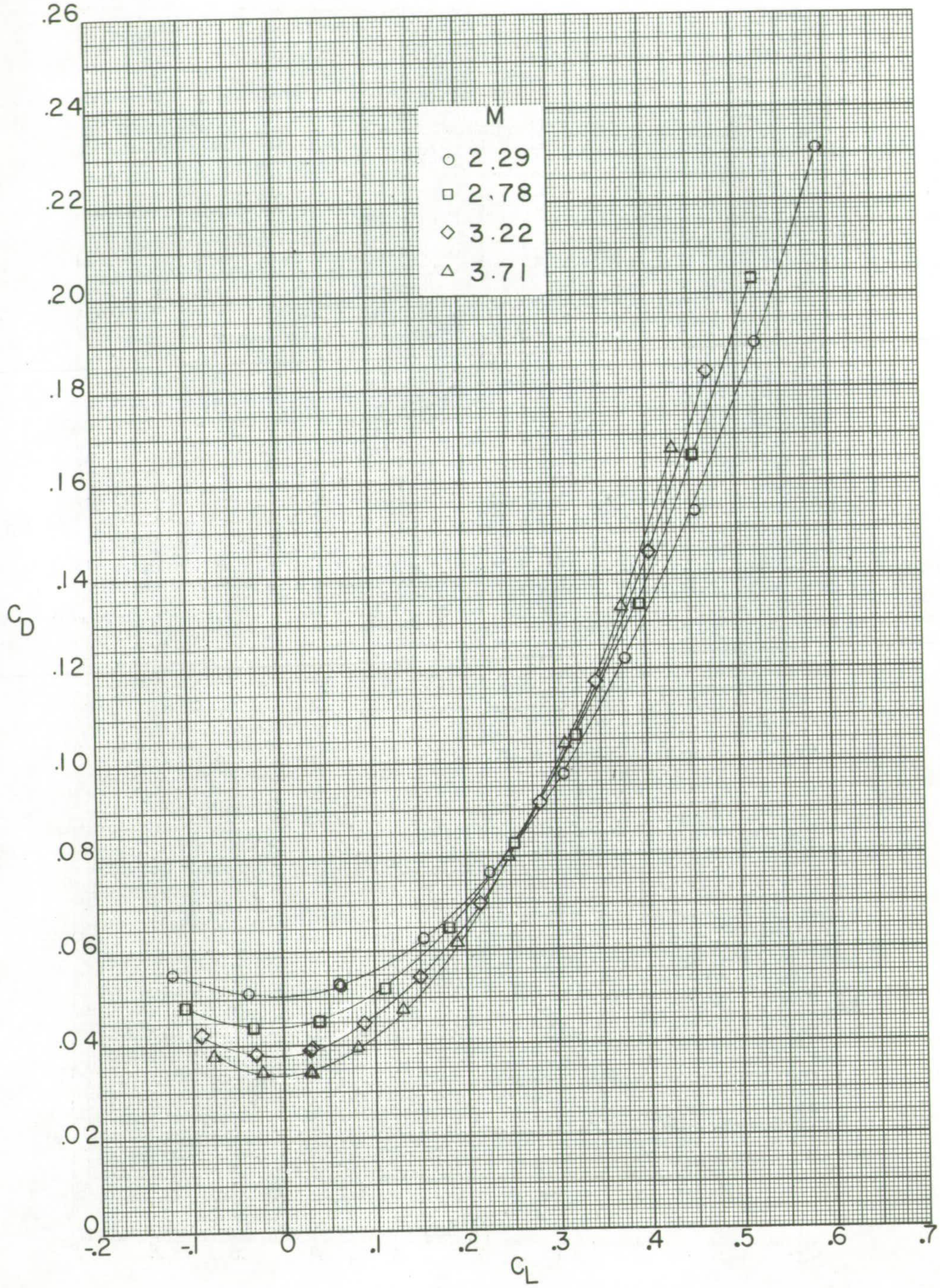

(b) Concluded.

Figure 6.- Concluded.

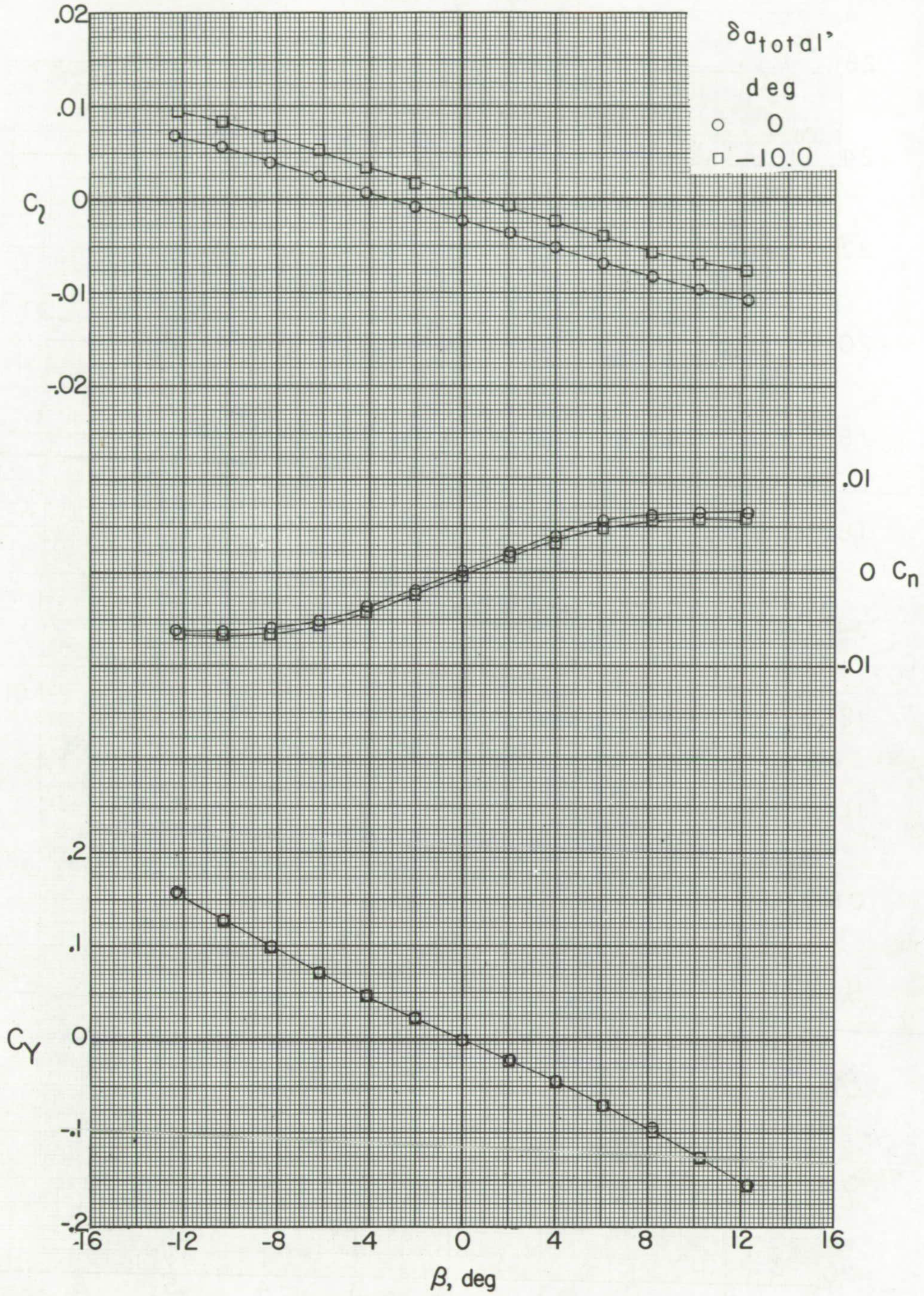

(a) $\alpha = 0.2^{\circ}$.

Figure 7.- Aerodynamic characteristics in sideslip about the body axis of the 0.067-scale model of the Bell X-2 airplane. M = 2.29.

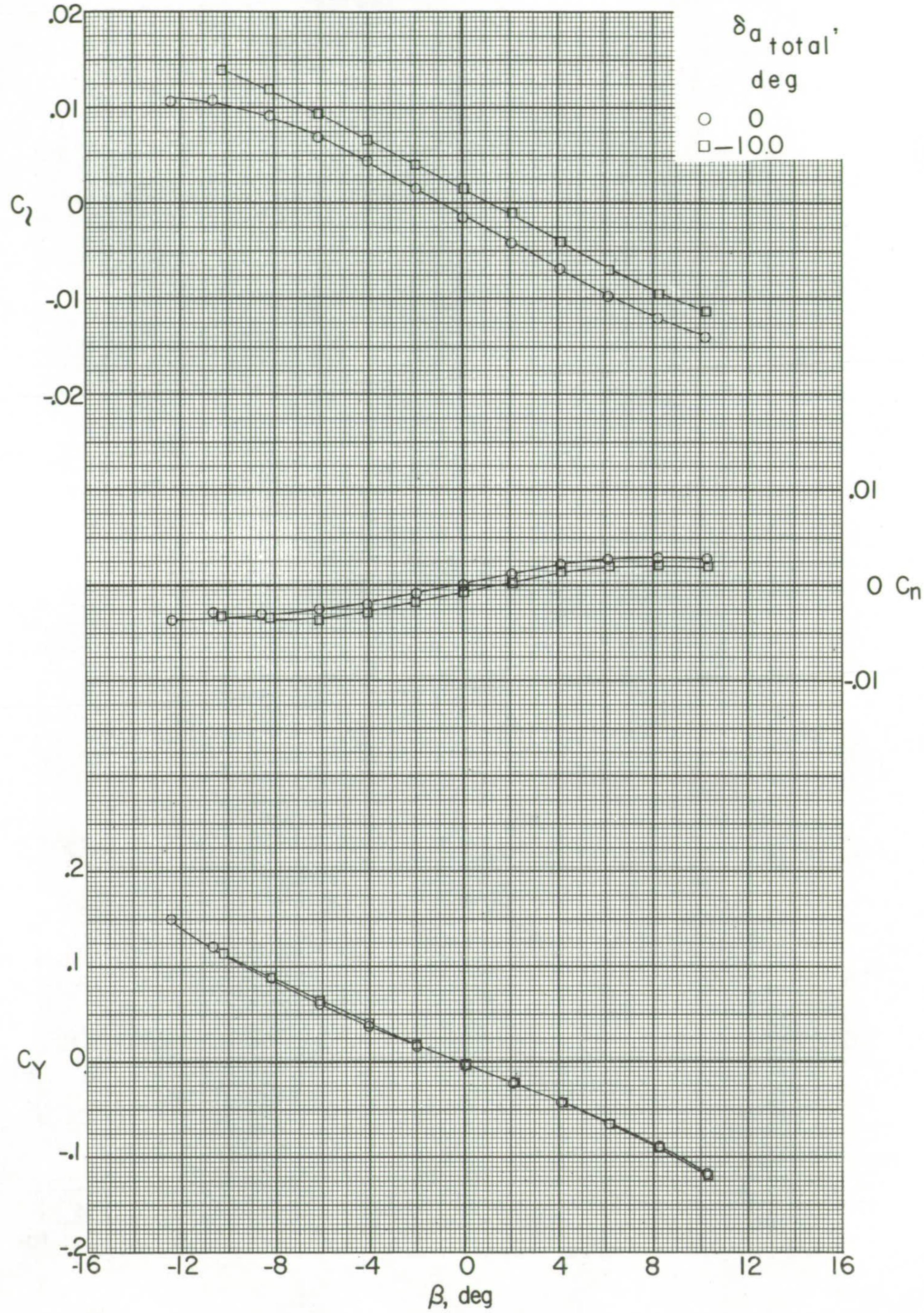

(b) $\alpha = 5.7^{\circ}$.

Figure 7.- Continued.

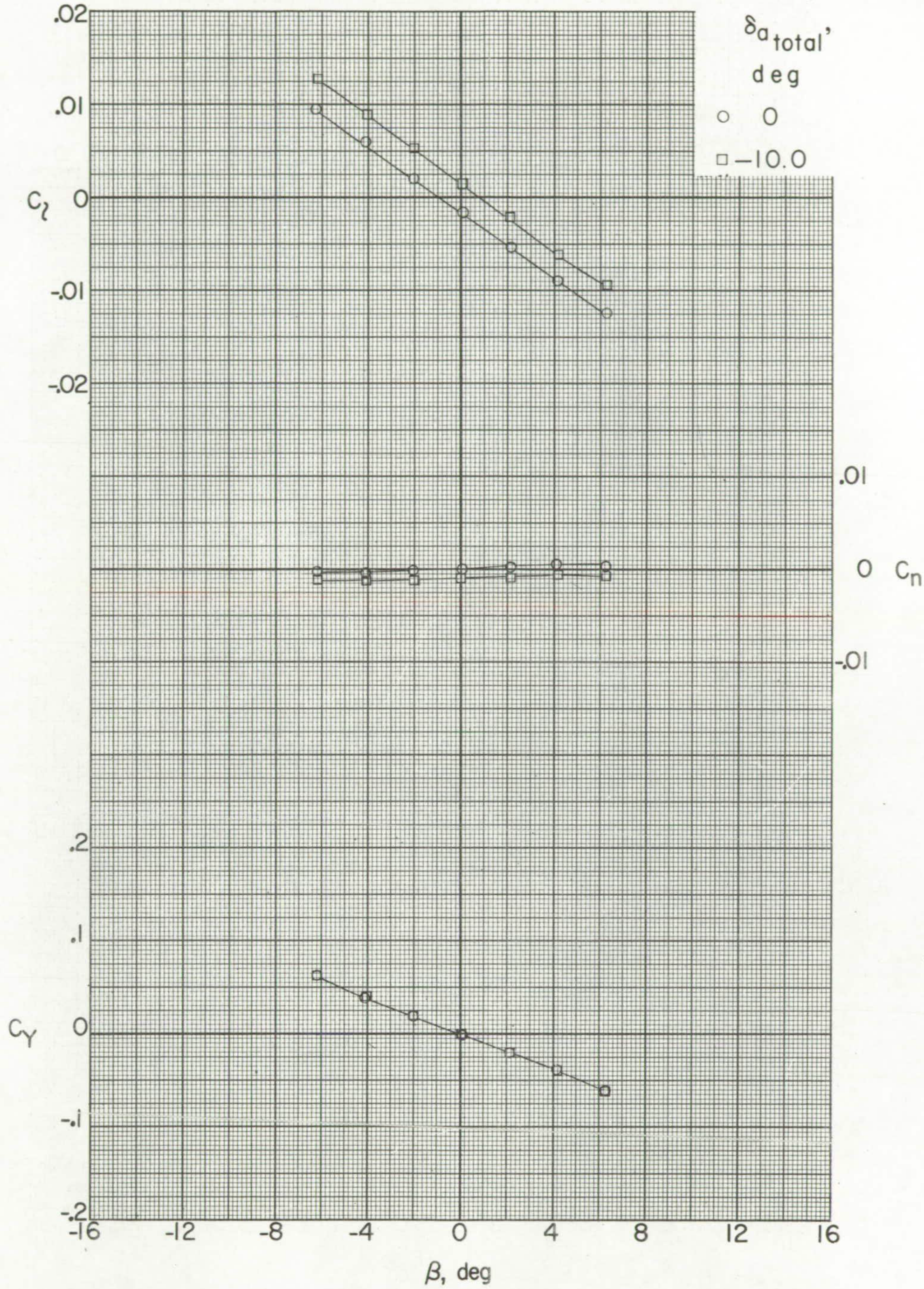

(c) $\alpha = 11.0^{\circ}$.

Figure 7.- Concluded.

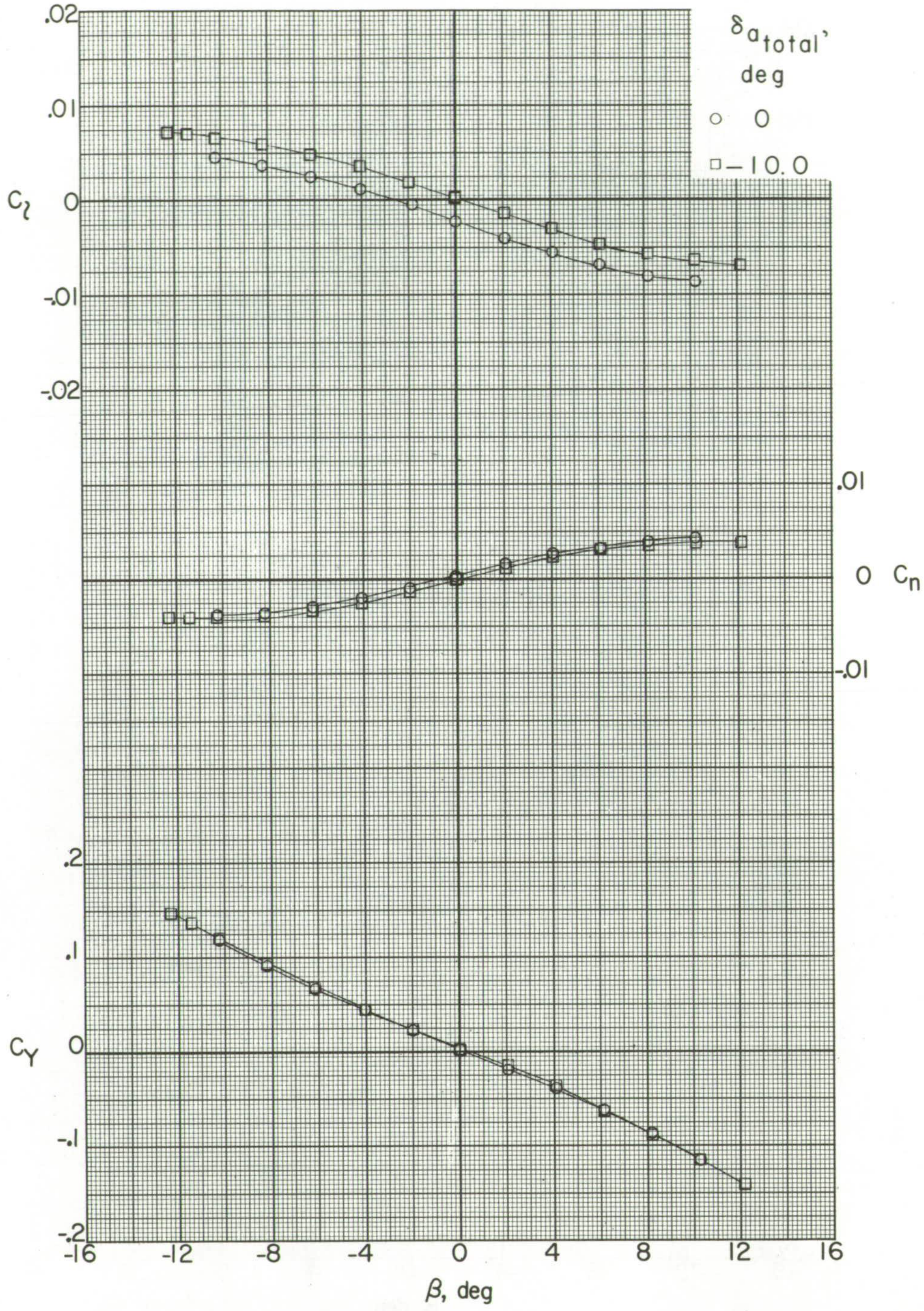

(a) $\alpha = 0.1^{\circ}$.

Figure 8.- Aerodynamic characteristics in sideslip about the body axis of the 0.067-scale model of the Bell X-2 airplane. M = 2.78.

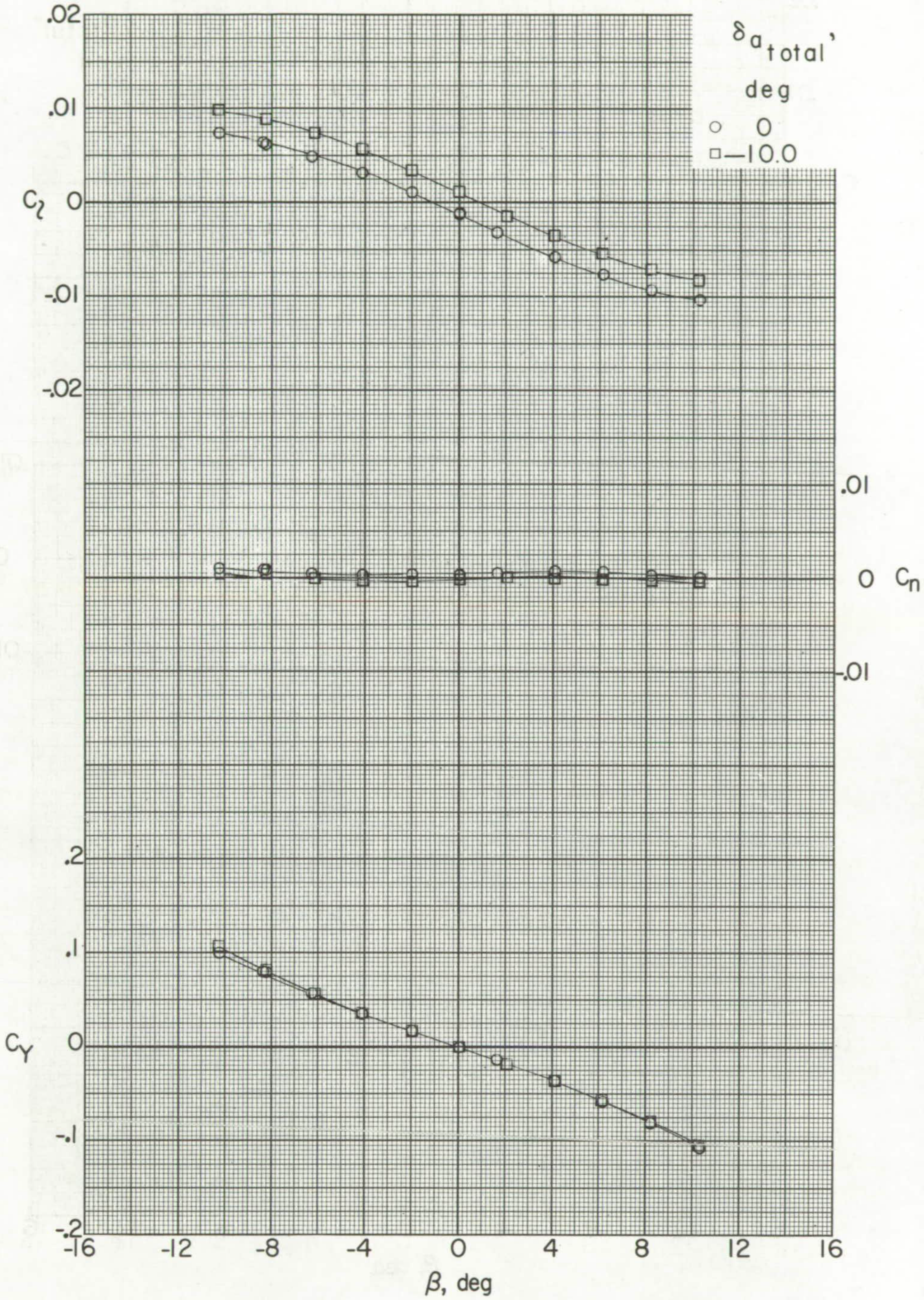

(b) $\alpha = 5.5^{\circ}$.

Figure 8.- Continued.

[redacted]

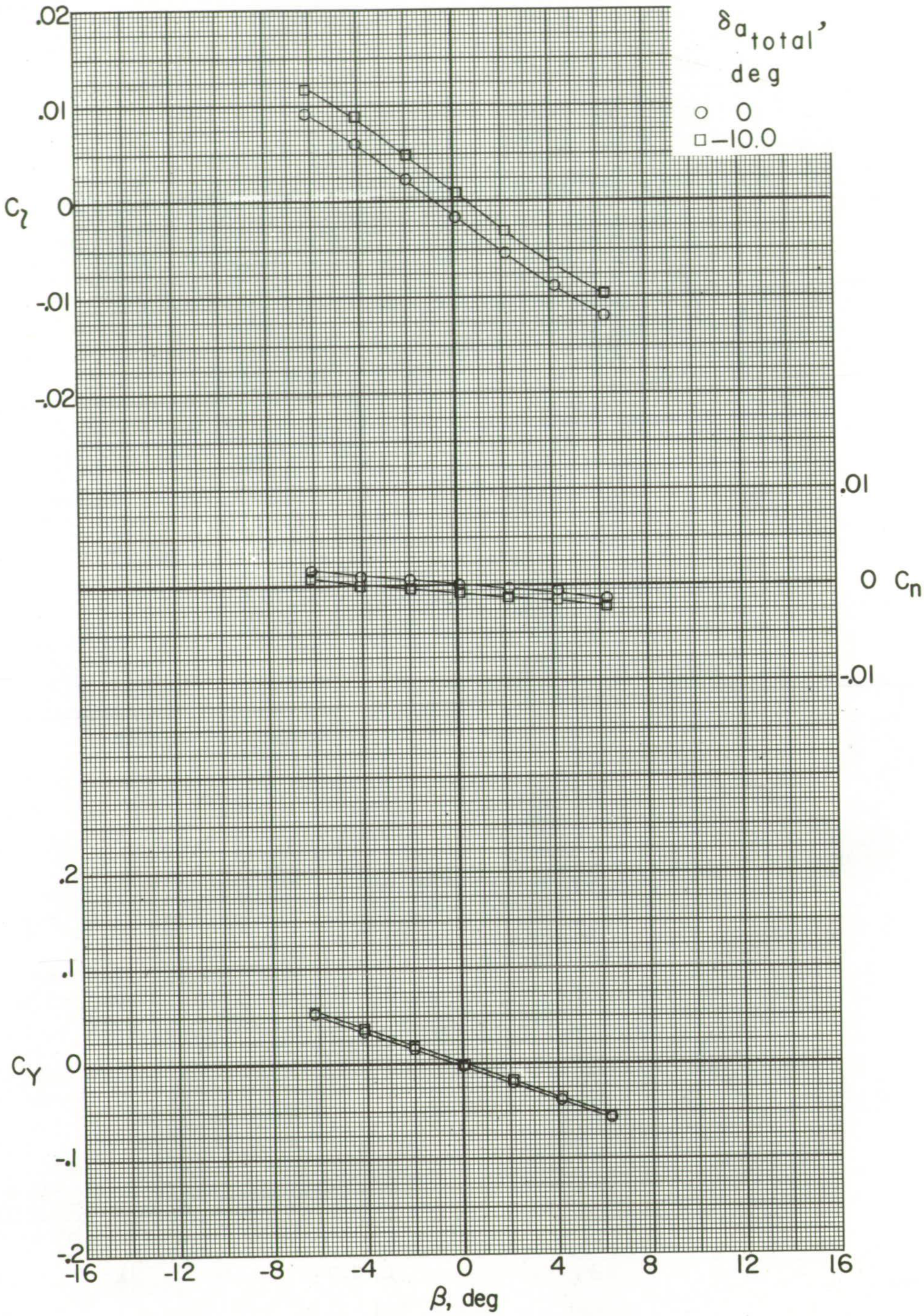

(c) $\alpha = 10.8^{\circ}$.

Figure 8.- Concluded.

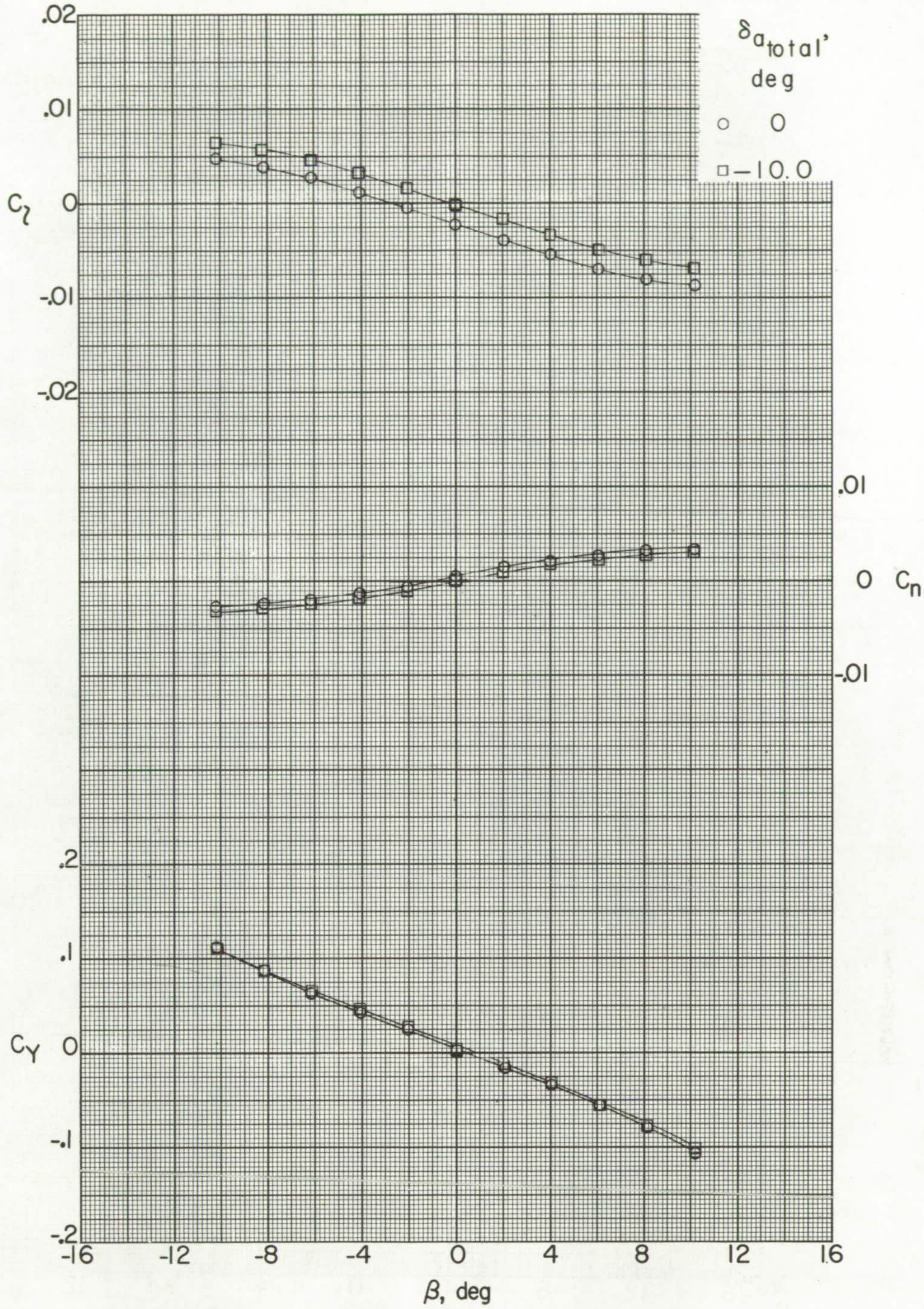

(a) $\alpha = 0.1^{\circ}$.

Figure 9.- Aerodynamic characteristics in sideslip about the body axis of the 0.067-scale model of the Bell X-2 airplane. M = 3.22.

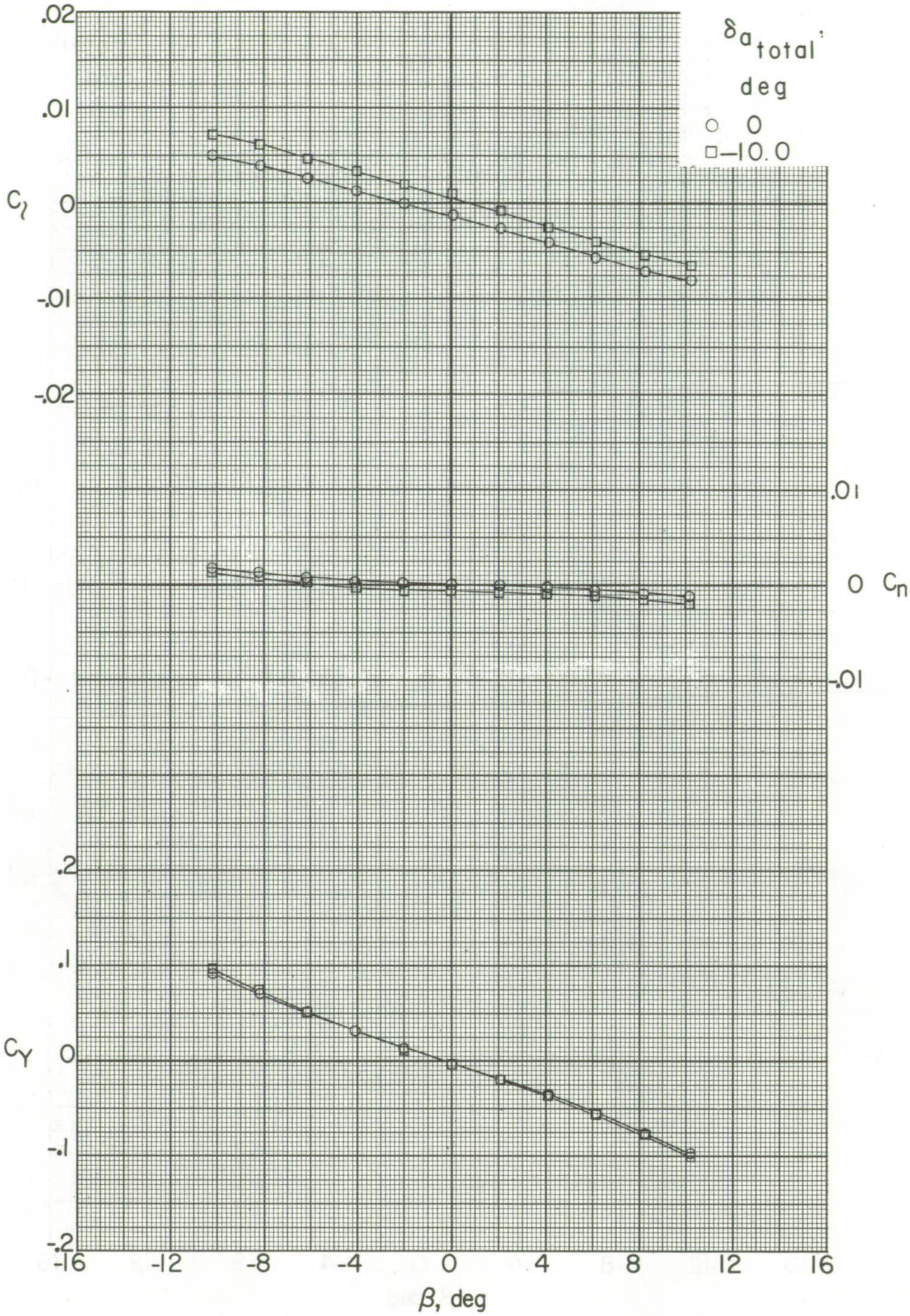

(b) $\alpha = 5.4^{\circ}$.

Figure 9.- Continued.

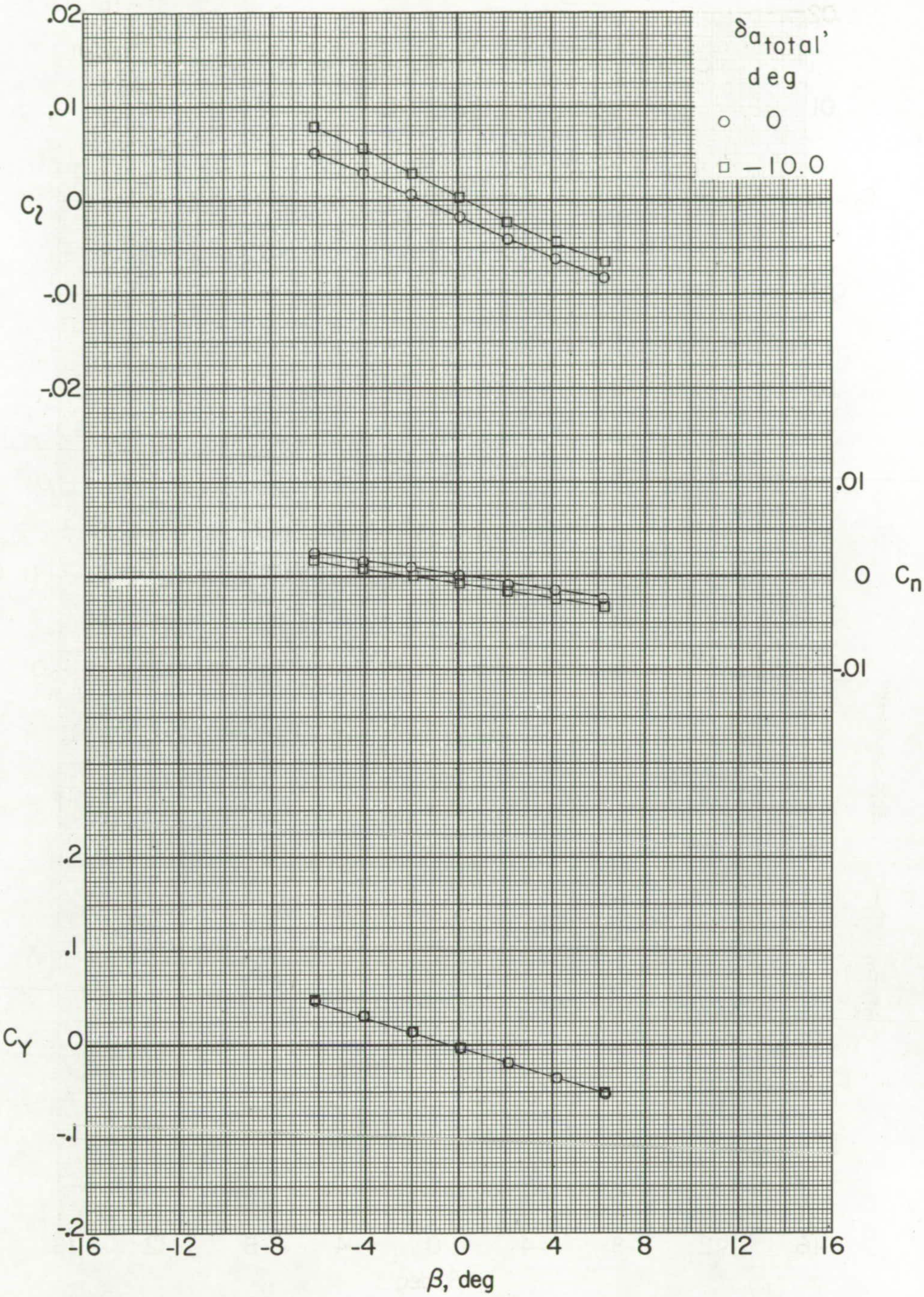

(c) $\alpha = 10.6^{\circ}$.

Figure 9.- Concluded.

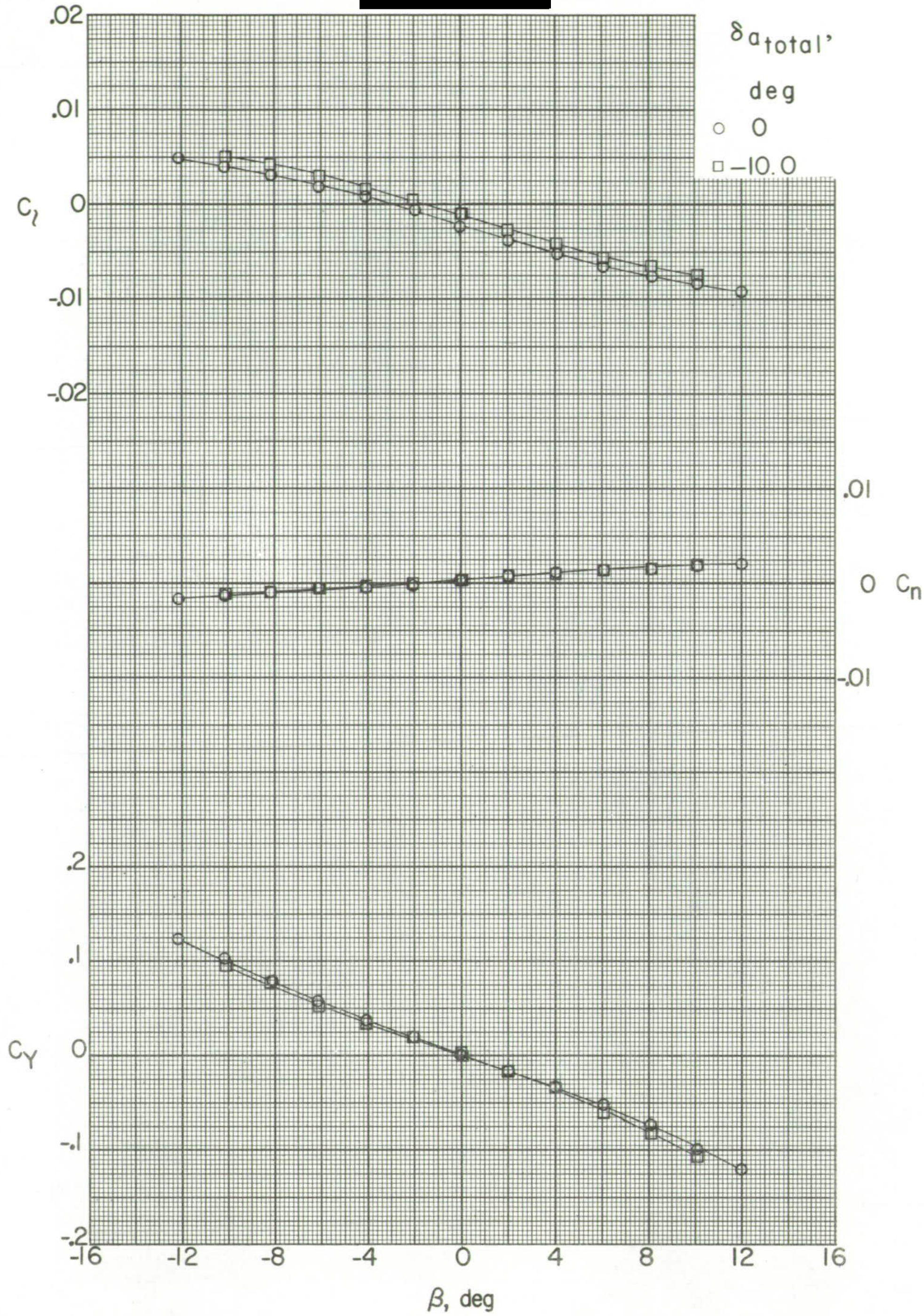

(a) $\alpha = 0^{\circ}$.

Figure 10.- Aerodynamic characteristics in sideslip about the body axis of the 0.067-scale model of the Bell X-2 airplane. M = 3.71.

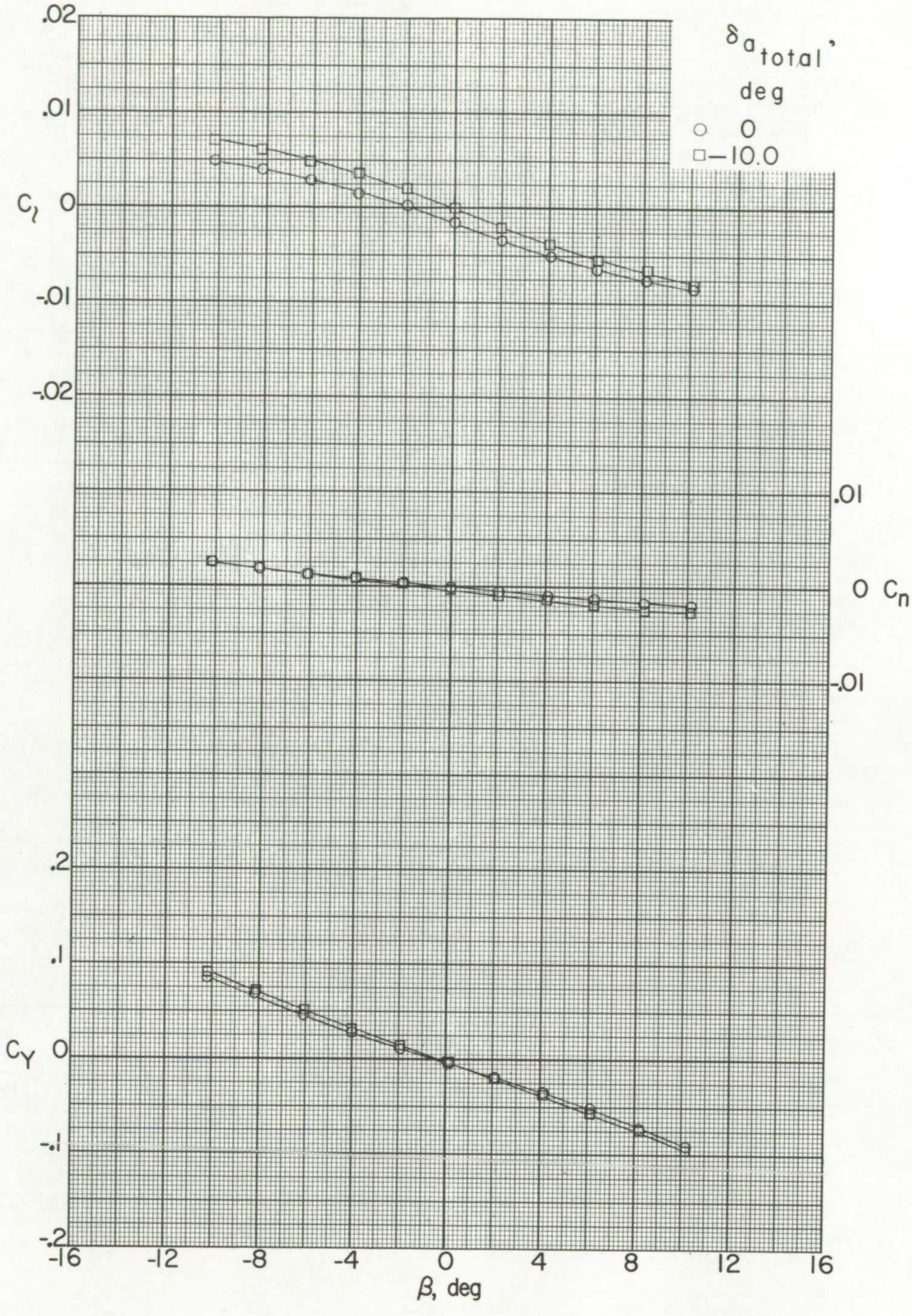

(b) $\alpha = 5.3^{\circ}$.

Figure 10.- Continued.

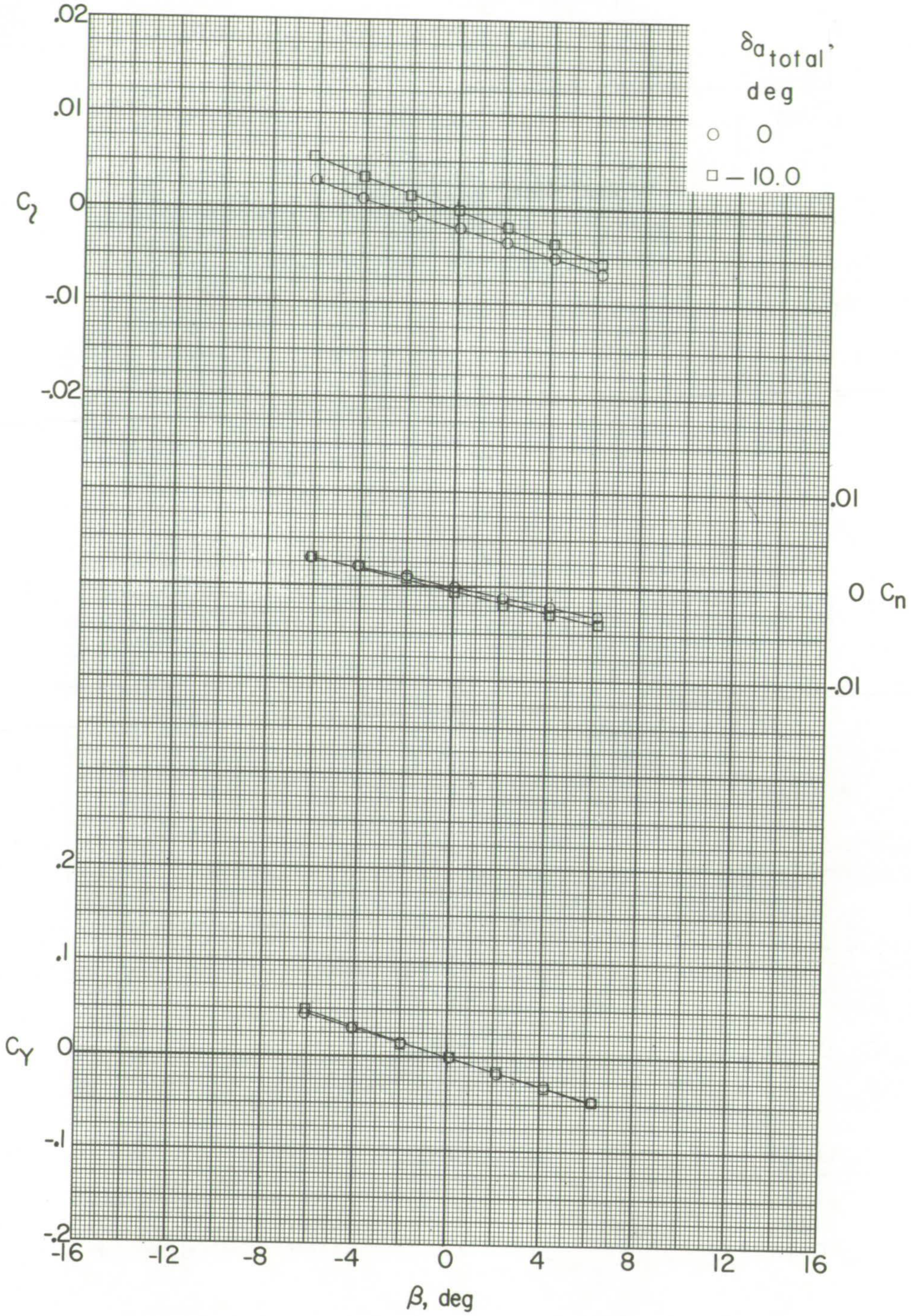

(c) $\alpha = 10.5^{\circ}$.

Figure 10.- Concluded.

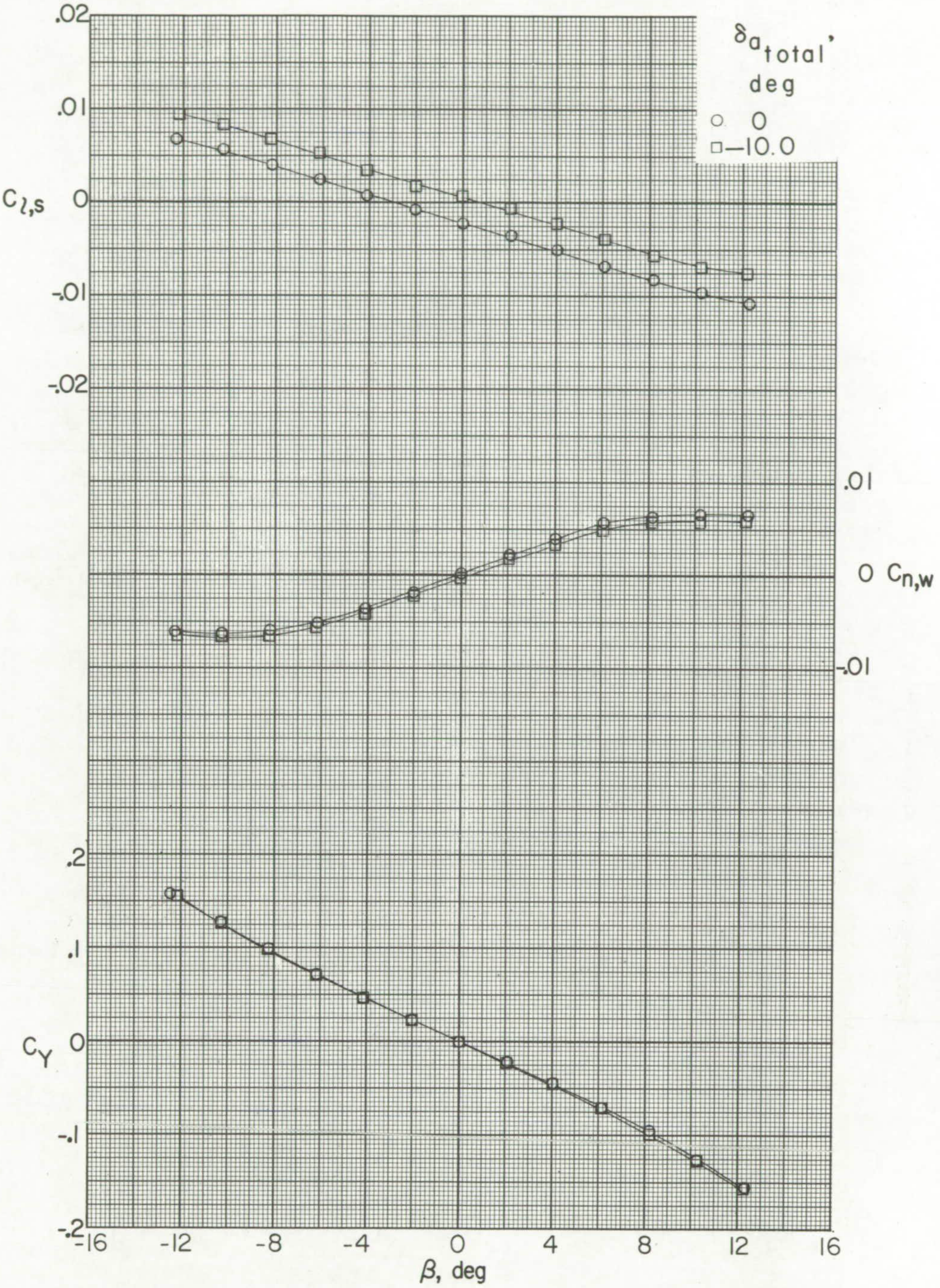

(a) $\alpha = 0.2^{\circ}$.

Figure 11.- Aerodynamic characteristics in sideslip about the stability axis of the 0.067-scale model of the Bell X-2 airplane. M = 2.29.

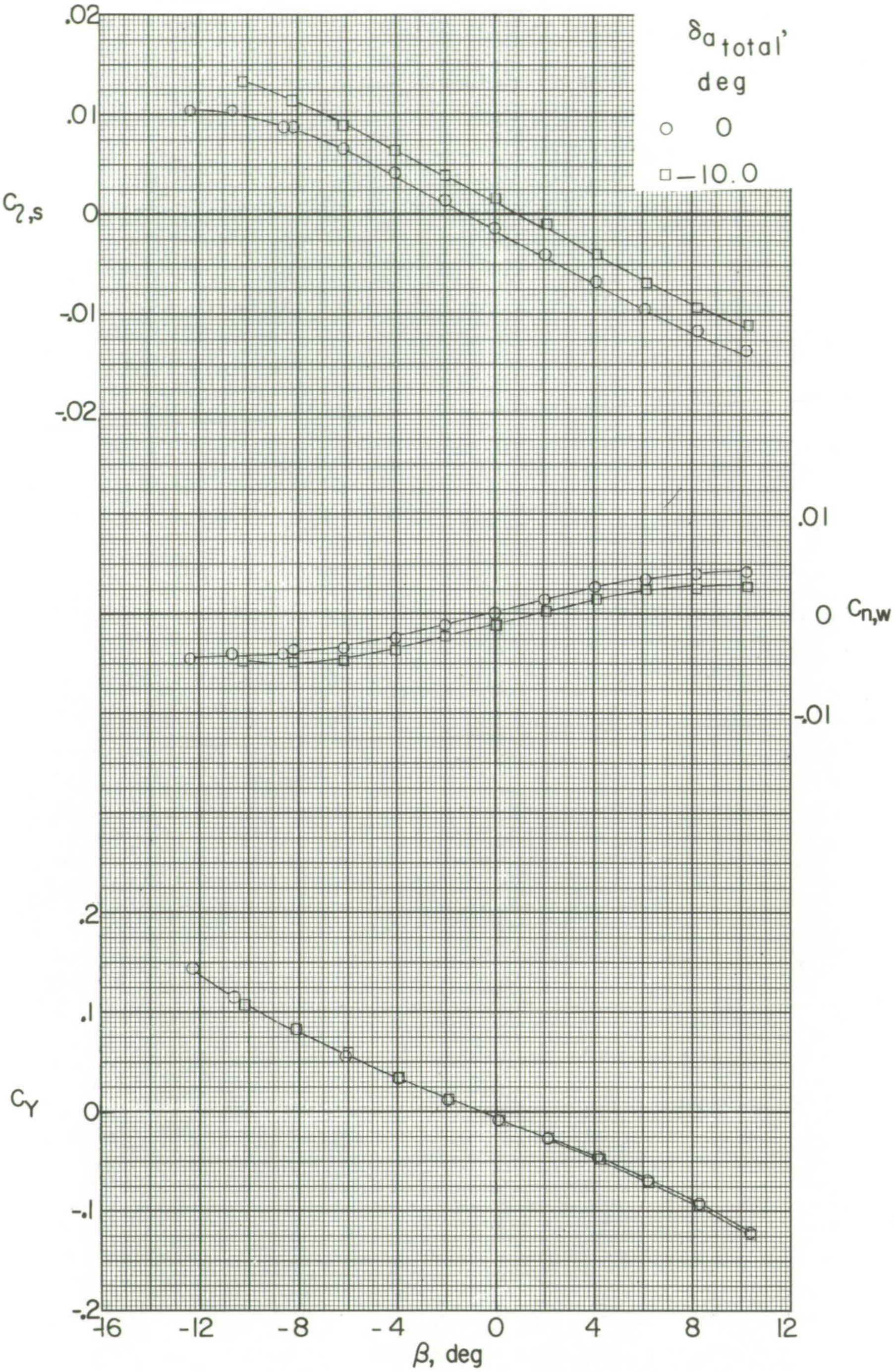

(b) $\alpha = 5.7^{\circ}$.

Figure 11.- Continued.

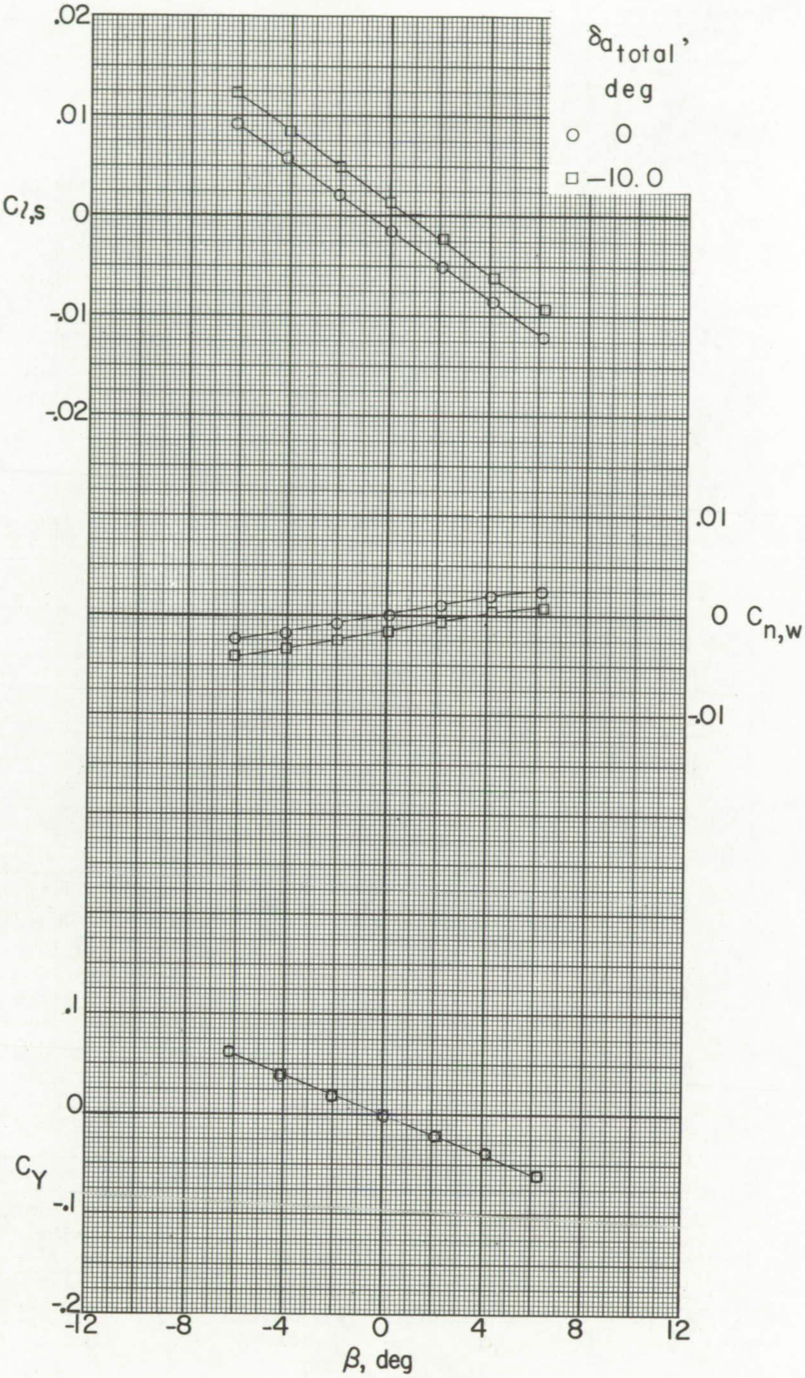

(c) $\alpha = 11.0^{\circ}$.

Figure 11.- Concluded.

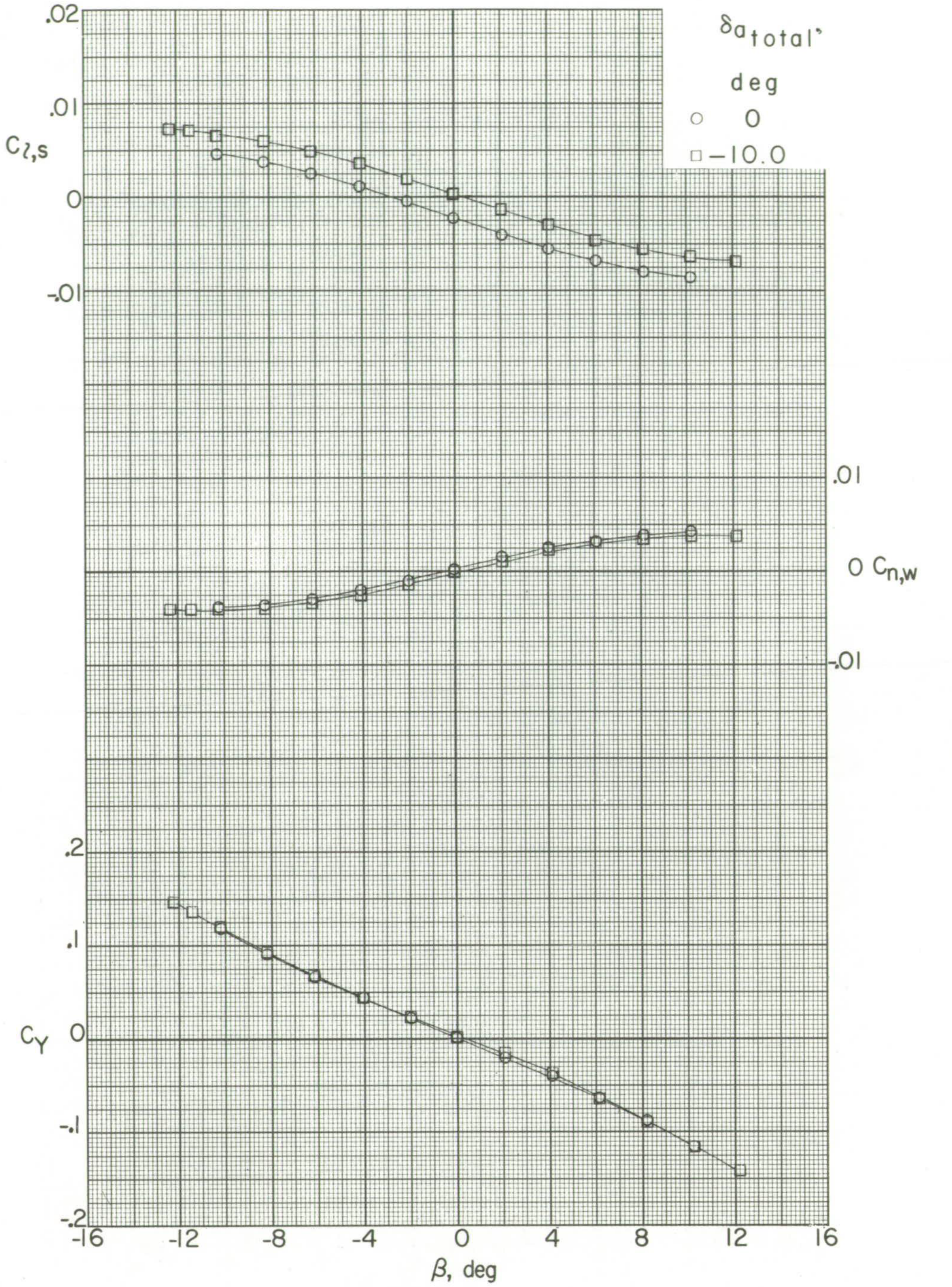

(a) $\alpha = 0.1^{\circ}$.

Figure 12.- Aerodynamic characteristics in sideslip about the stability axis of the 0.067-scale model of the Bell X-2 airplane. M = 2.78.

[redacted]

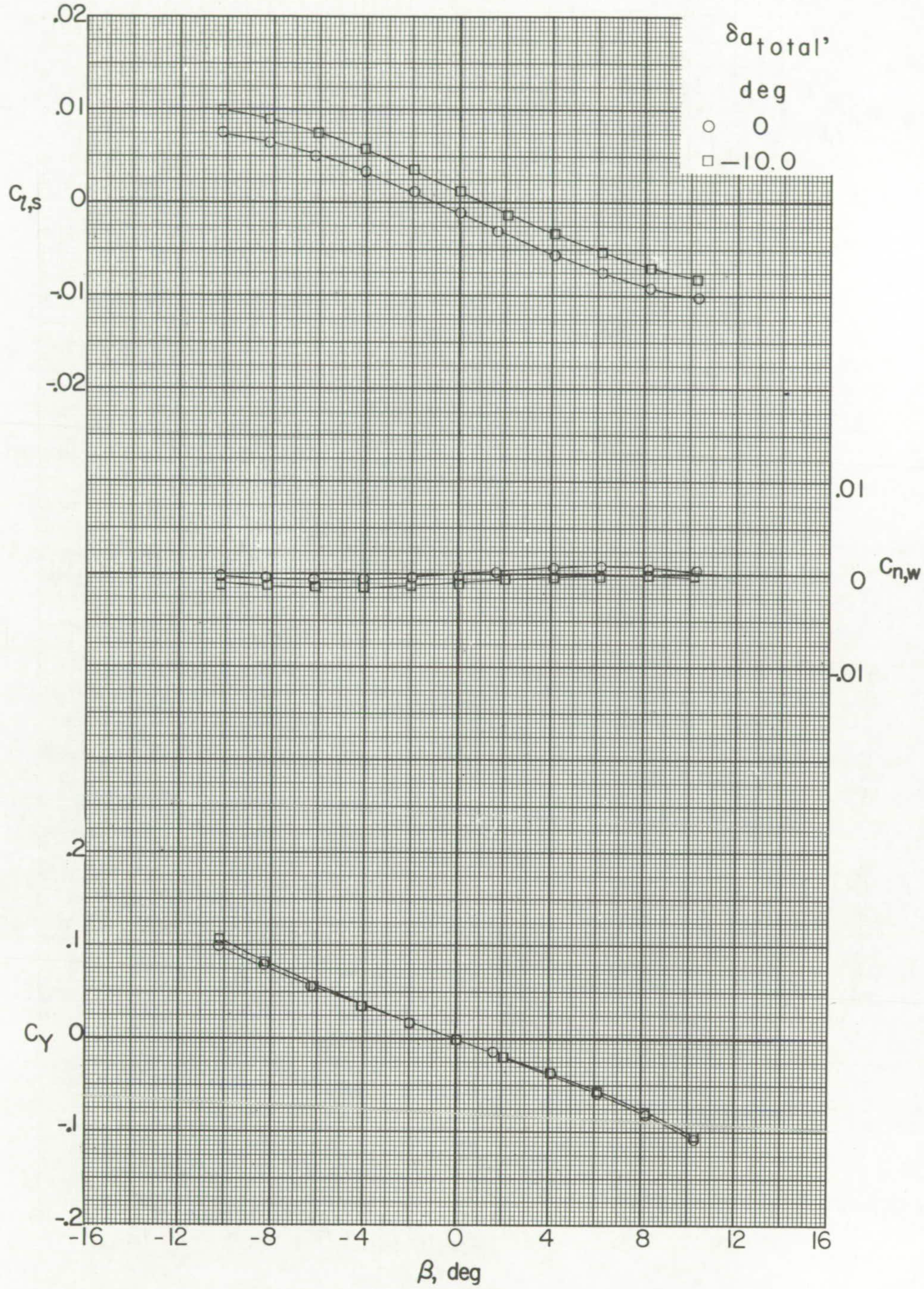

(b) $\alpha = 5.5^{\circ}$.

Figure 12.- Continued.

[redacted]

[redacted]

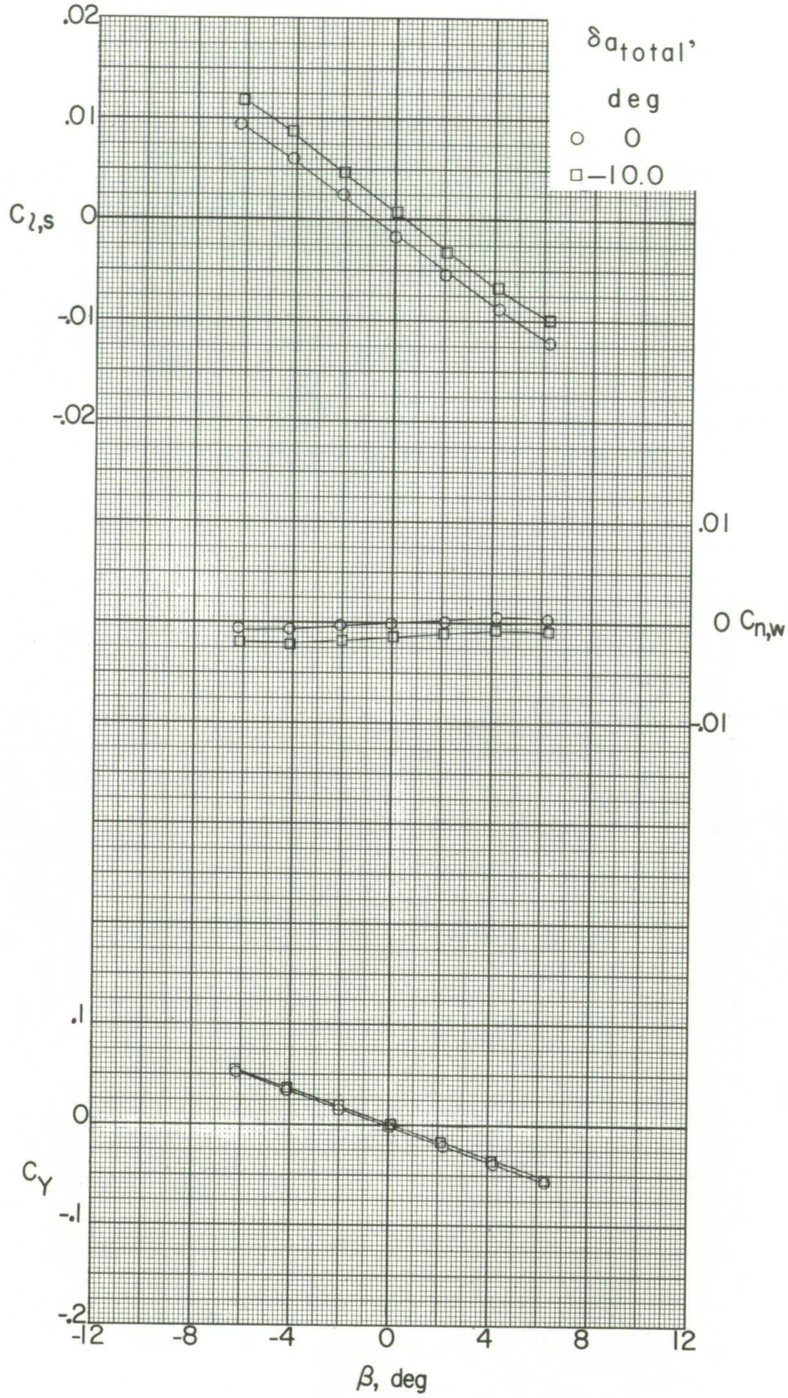

(c) $\alpha = 10.8^{\circ}$.

Figure 12.- Concluded.

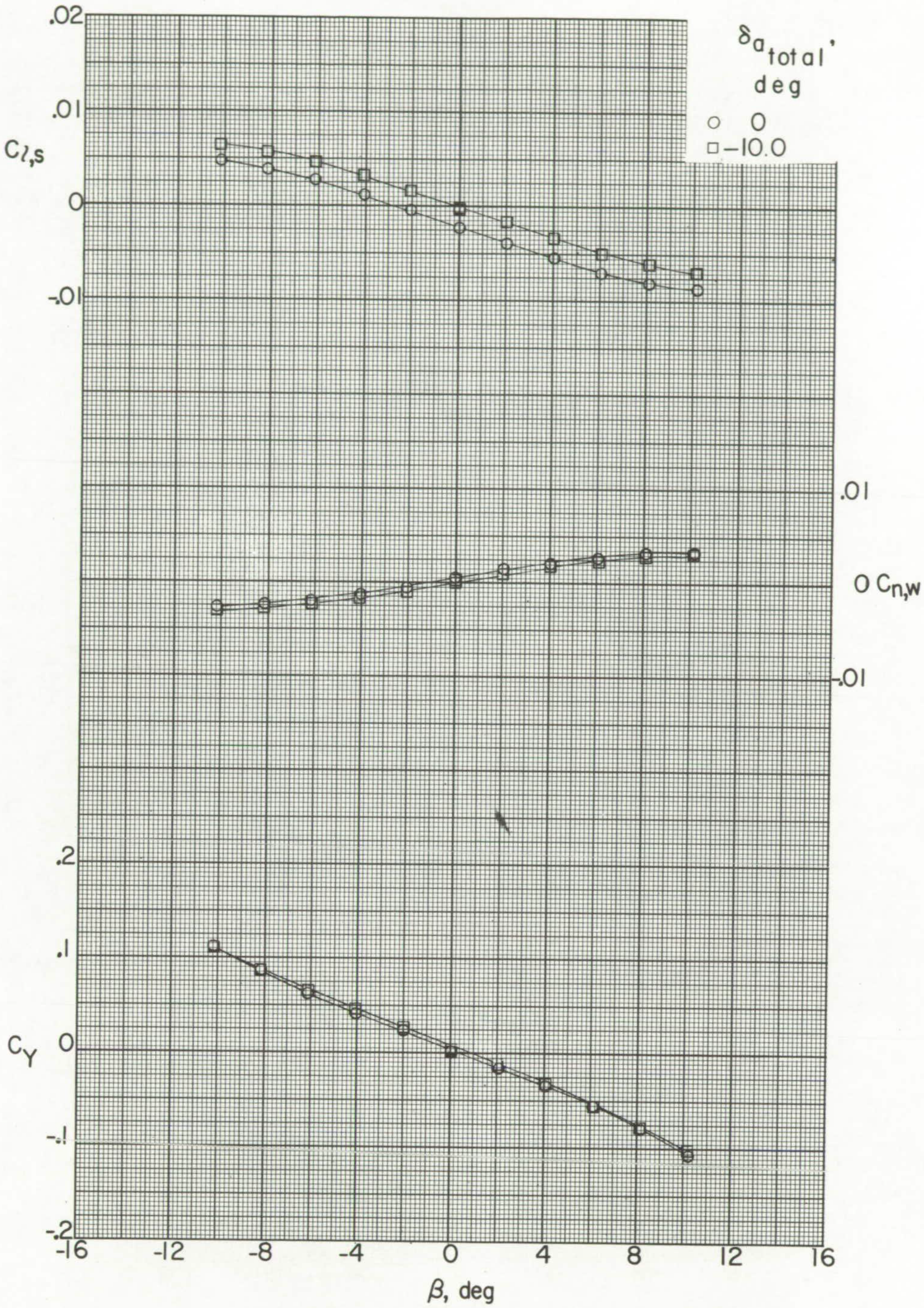

(a) $\alpha = 0.1^{\circ}$.

Figure 13.- Aerodynamic characteristics in sideslip about the stability axis of the 0.067-scale model of the Bell X-2 airplane. M = 3.22.

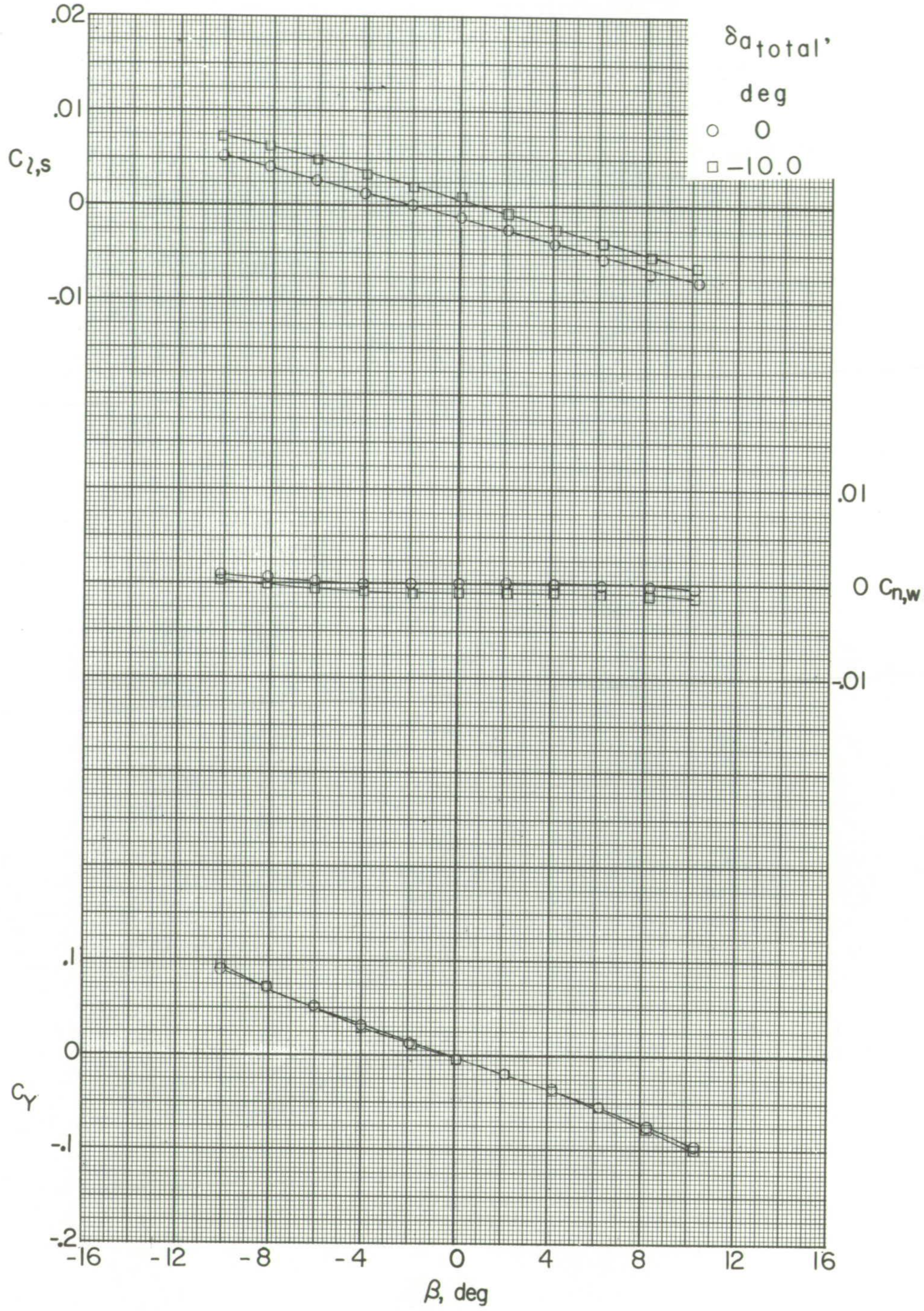

(b) $\alpha = 5.4^{\circ}$.

Figure 13.- Continued.

[redacted]

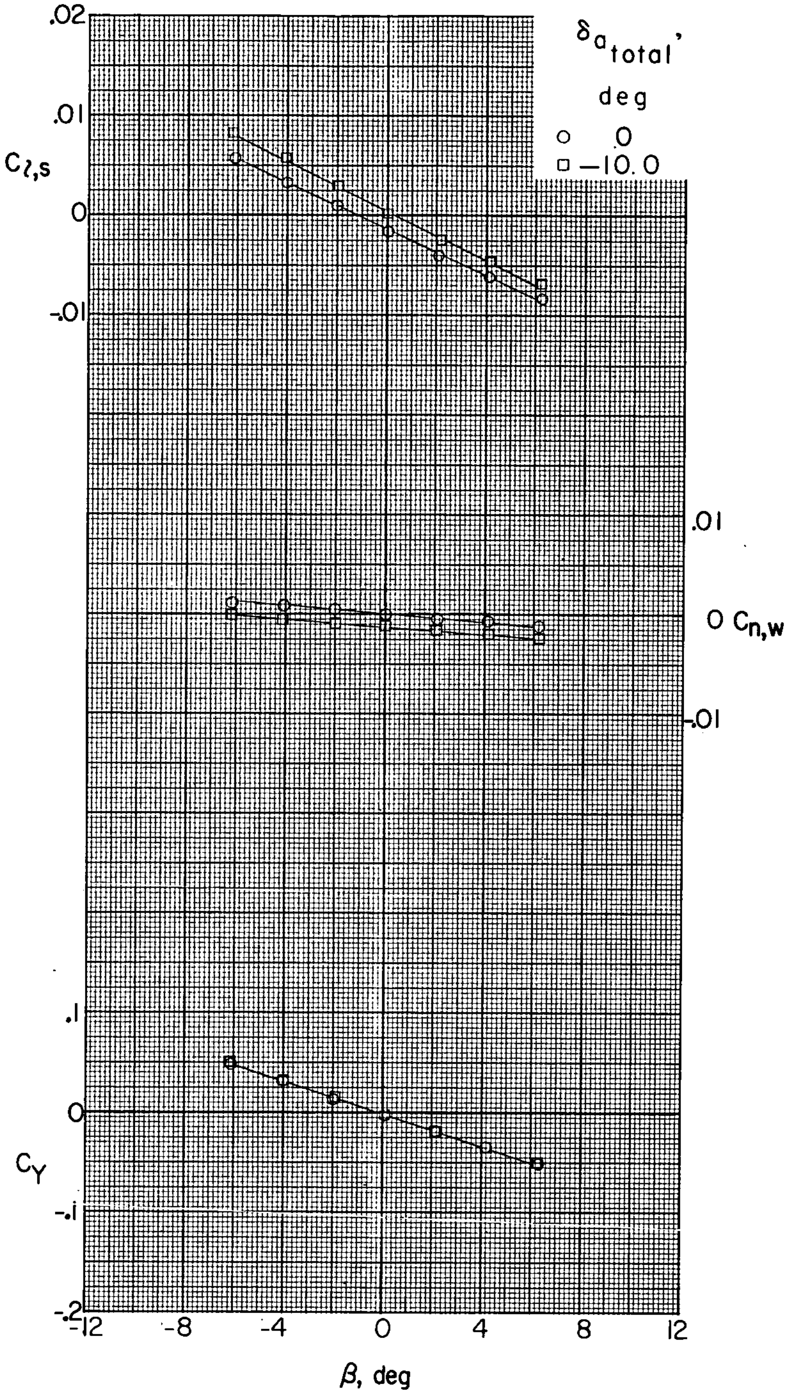

(c) $\alpha = 10.6^{\circ}$.

Figure 13.- Concluded.

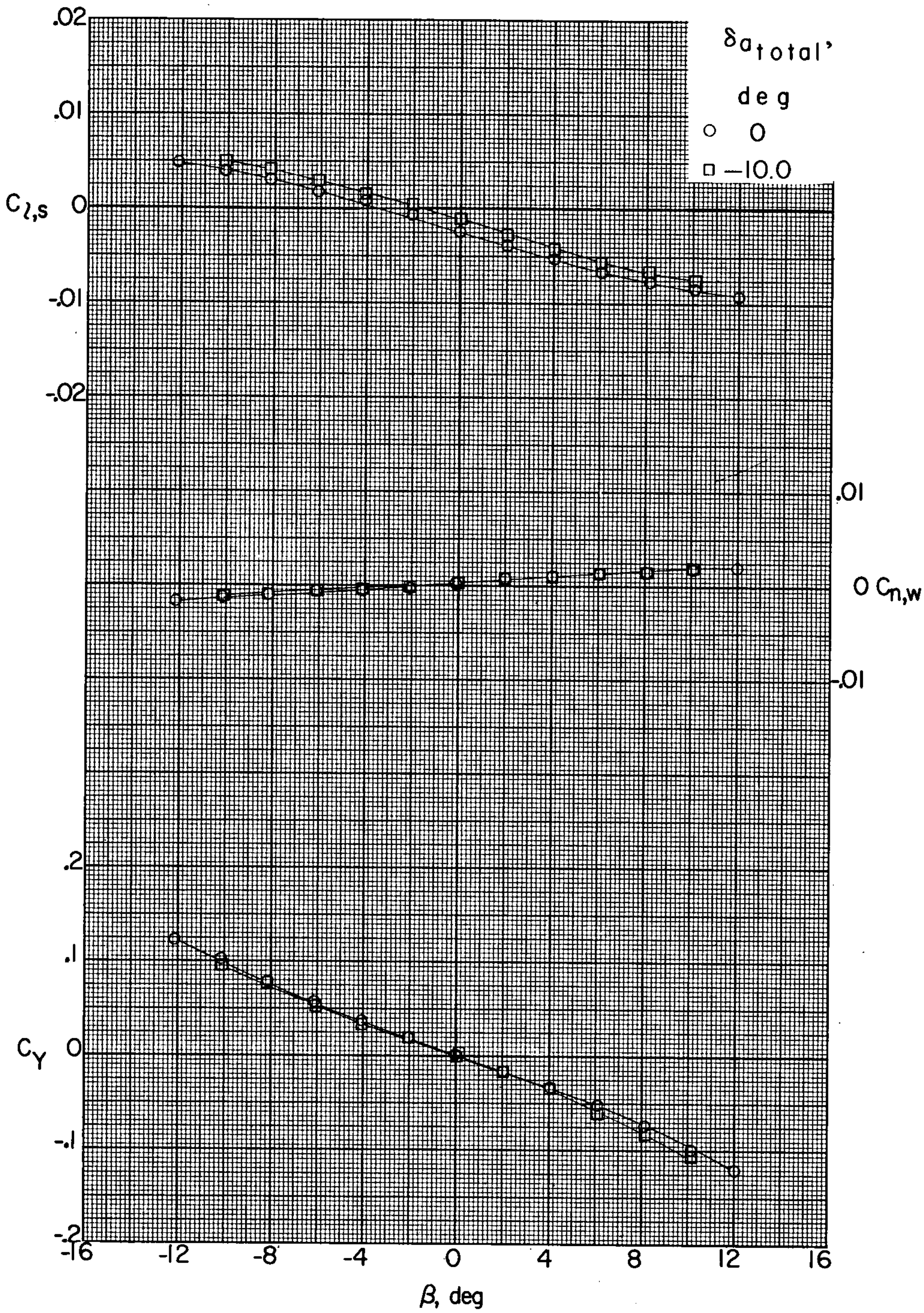

(a) $\alpha = 0^{\circ}$.

Figure 14.- Aerodynamic characteristics in sideslip about the stability axis of the 0.067-scale model of the Bell X-2 airplane. M = 3.71.

[redacted]

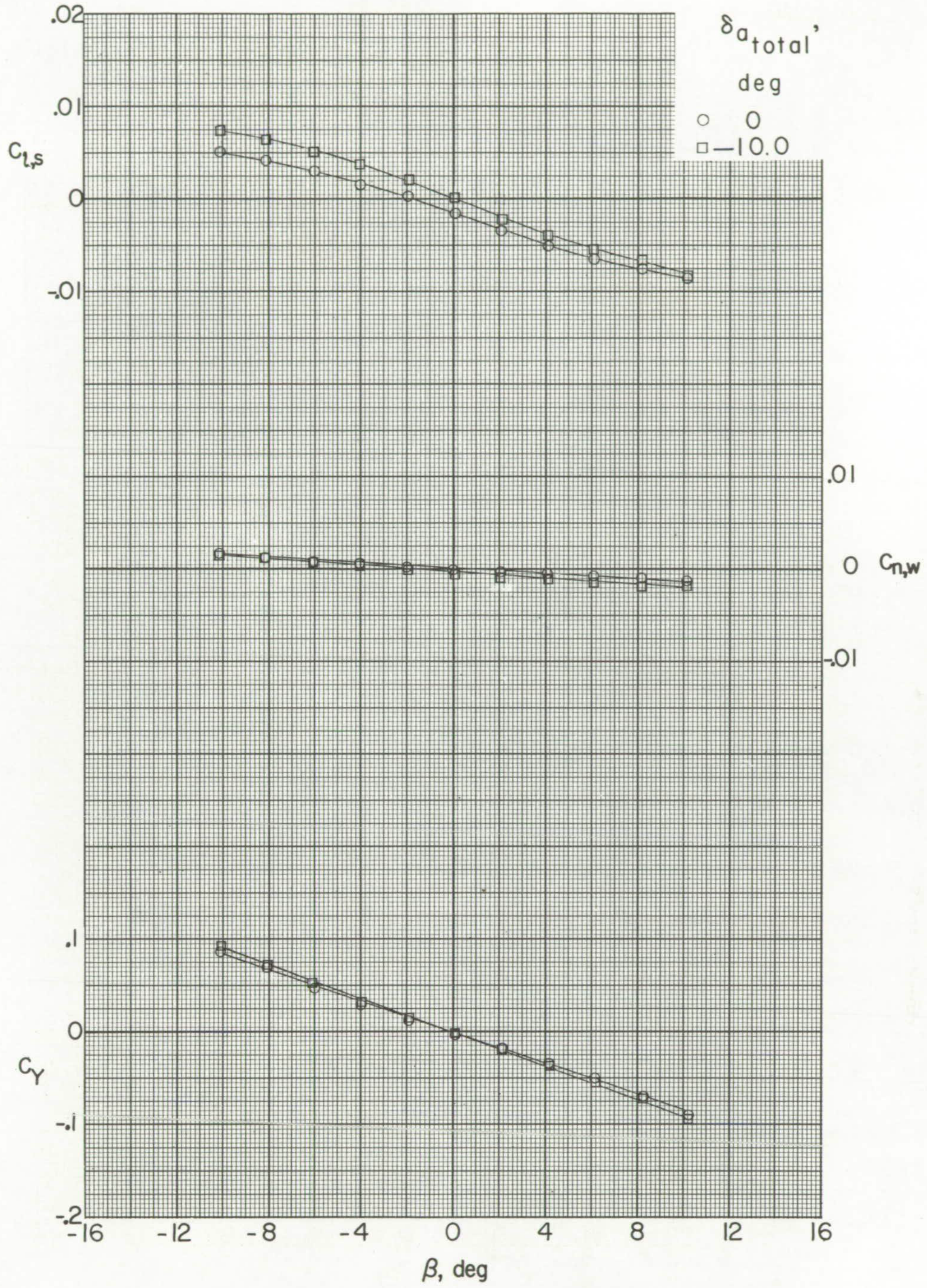

(b) $\alpha = 5.3^{\circ}$.

Figure 14.- Continued.

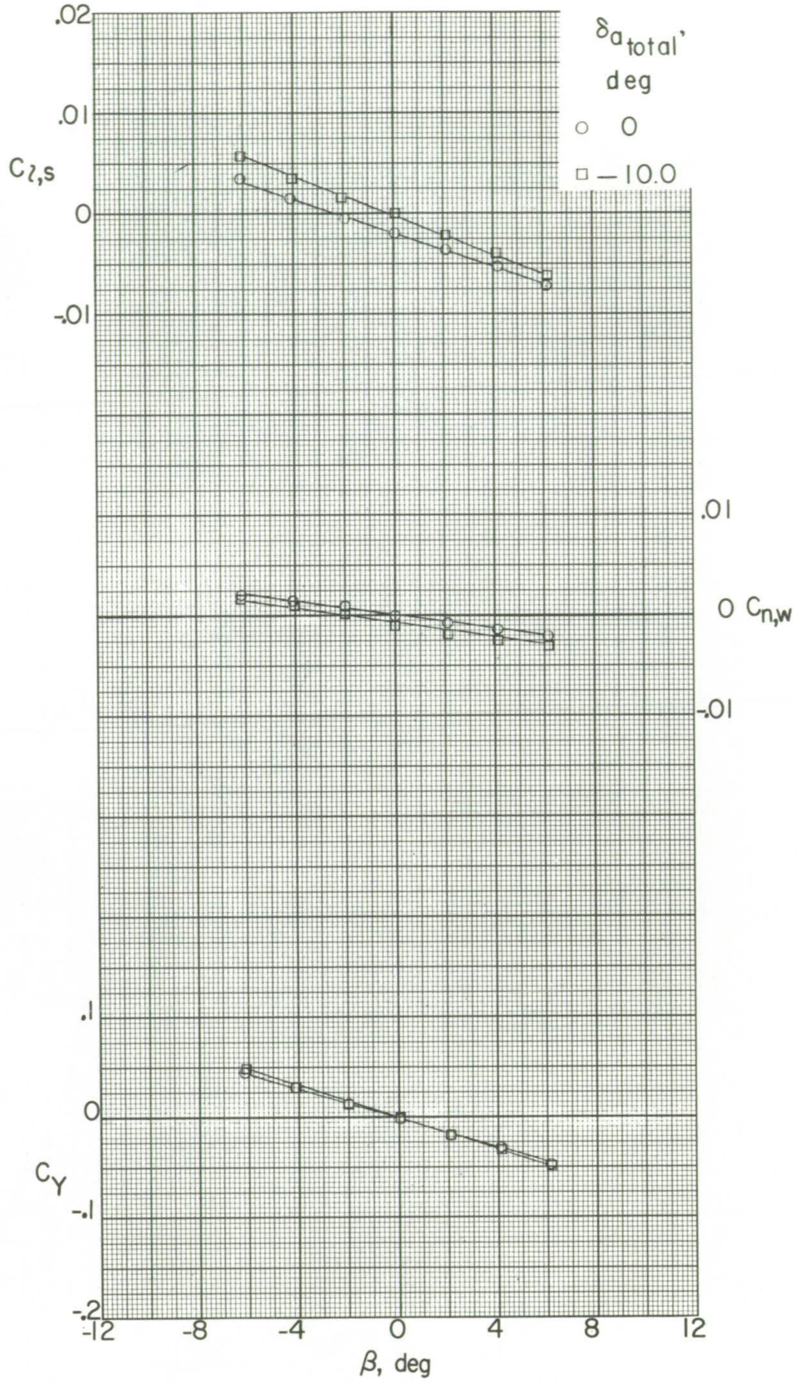

(c) $\alpha = 10.5^{\circ}$.

Figure 14.- Concluded.

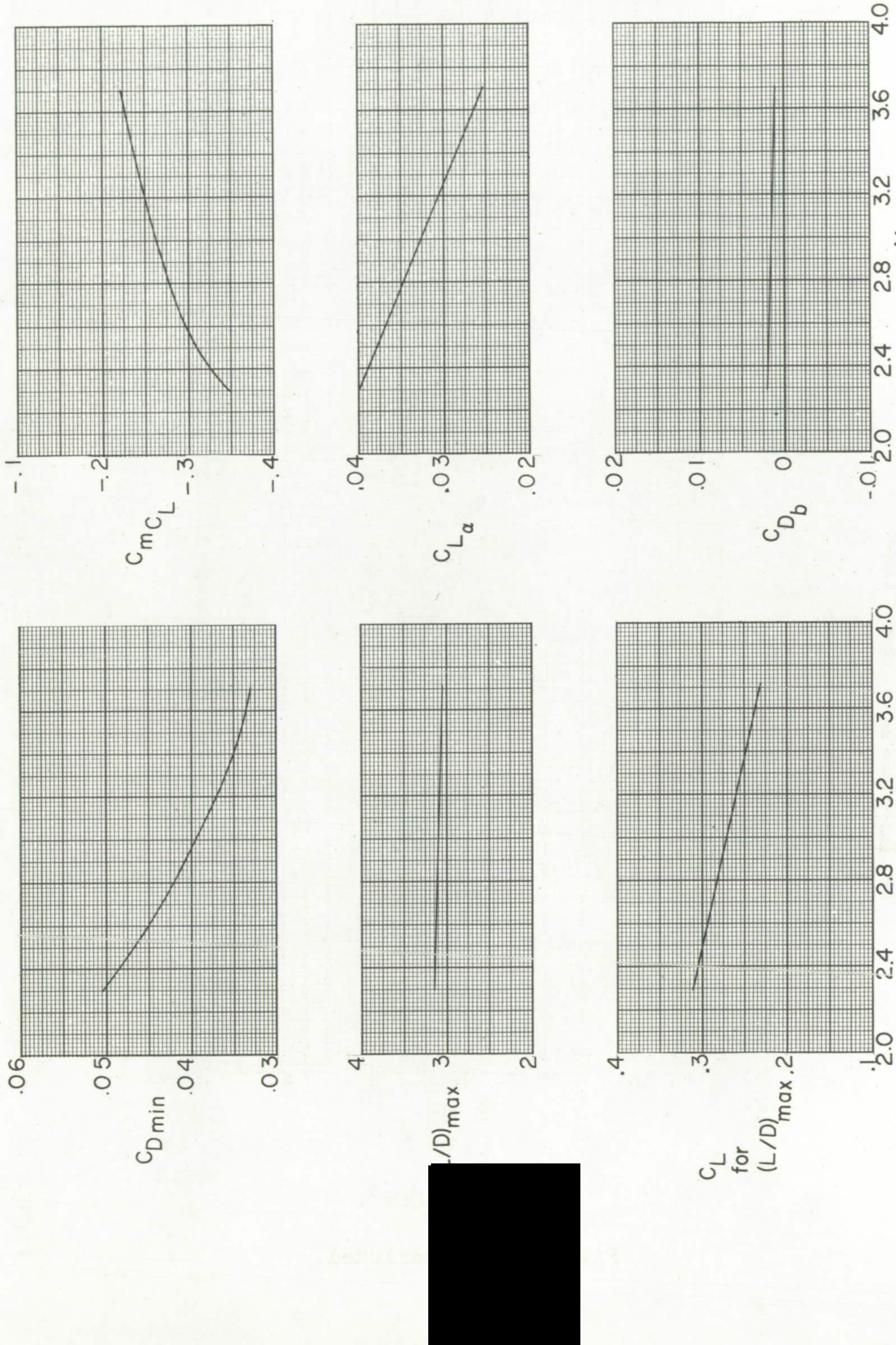

Figure 15.- Summary of the aerodynamic characteristics in pitch of the 0.067-scale model of the Bell X-2 airplane.

[redacted]

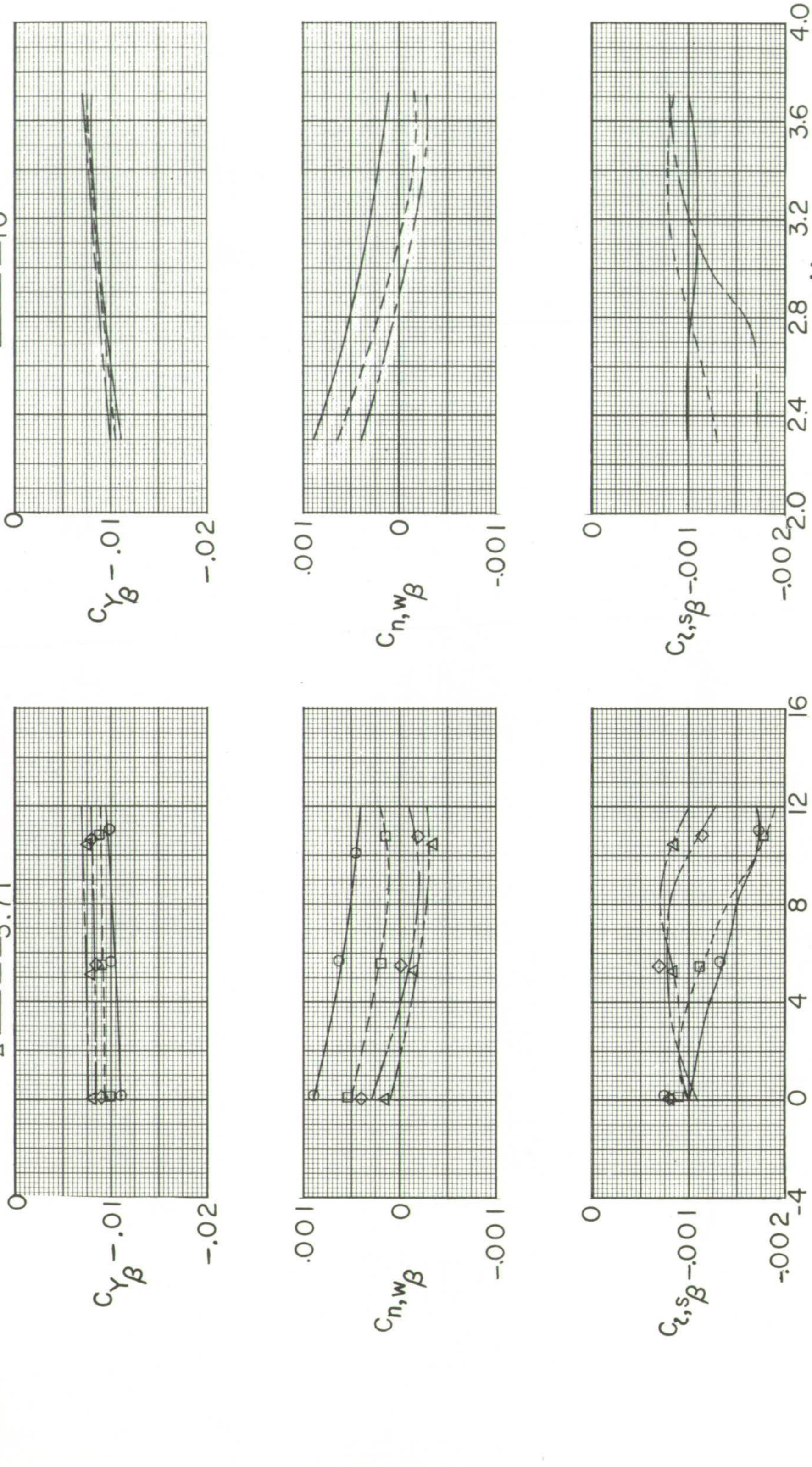

Figure 16.- Summary of the aerodynamic characteristics in sideslip about the stability axis of the 0.067-scale model of the Bell X-2 airplane.

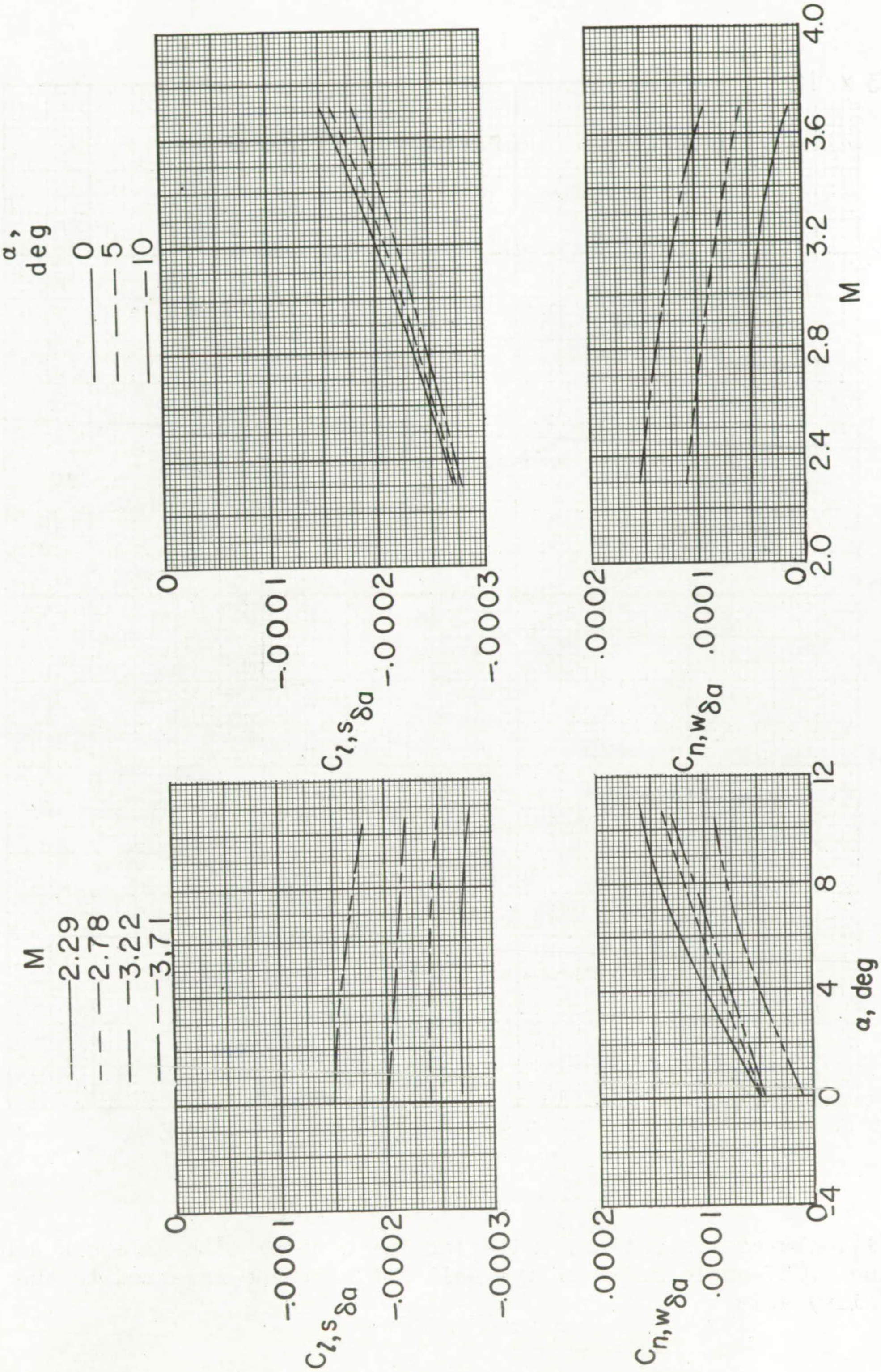

Figure 16.- Concluded.

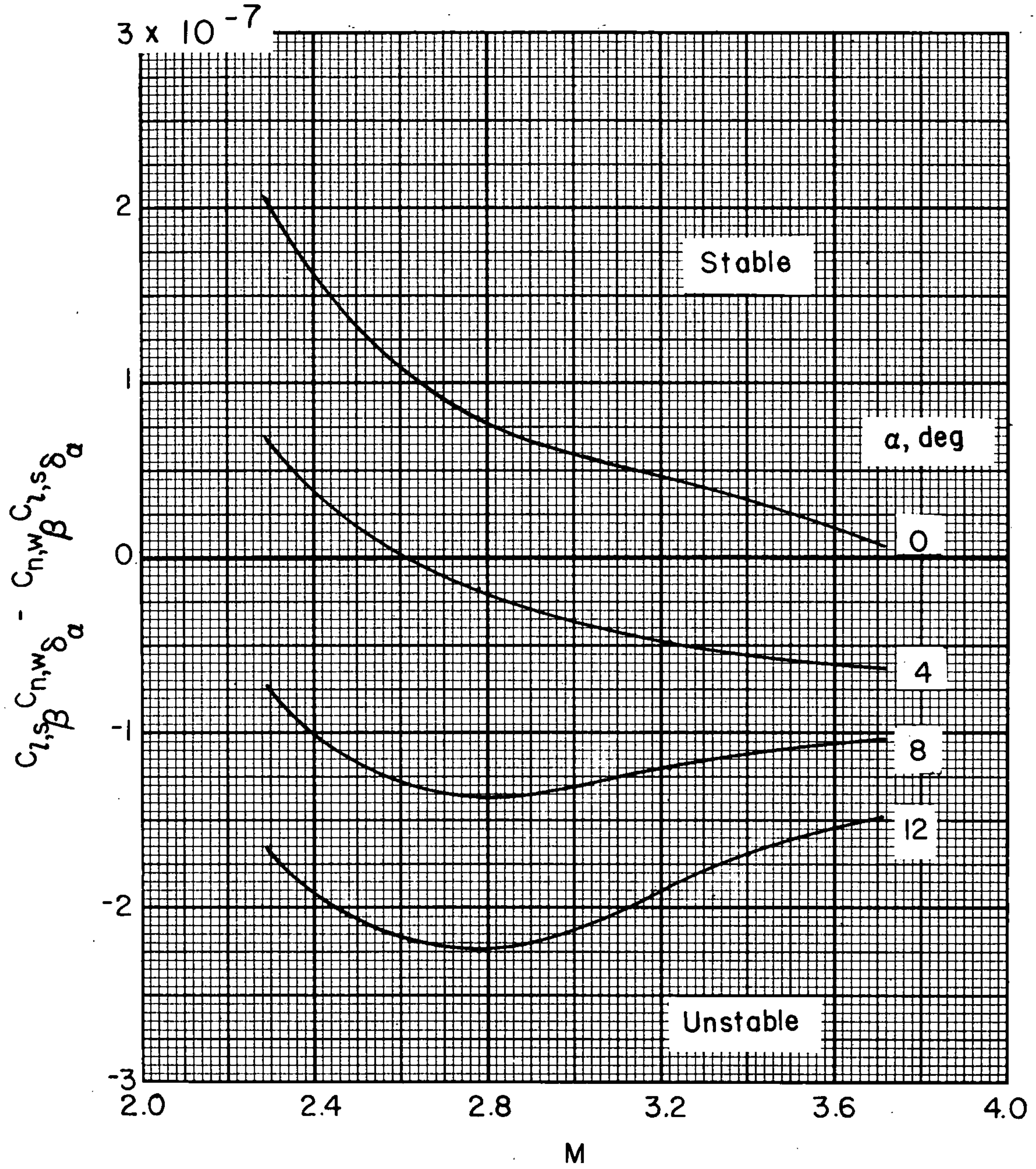

Figure 17.- Lateral stability criterion for control with ailerons alone of the 0.067-scale model of the Bell X-2 airplane referred to the stability axis.

[redacted]

[redacted]